

6716

NATIONAL LIBRARY  
OTTAWA



BIBLIOTHÈQUE NATIONALE  
OTTAWA

NAME OF AUTHOR... *HLING, ERIC KAM-LING* .....

TITLE OF THESIS... *SINGLE-CHANNEL N/D CALCULATION OF*  
*(i) TN & PARTIAL WAVES and*  
*(ii) EFFECTS OF INELASTICITY ON RESONANCES* .....

UNIVERSITY... *of ALBERTA EDMONTON* .....

DEGREE FOR WHICH THESIS WAS PRESENTED... *Ph.D* .....

YEAR THIS DEGREE GRANTED... *1970* .....

Permission is hereby granted to THE NATIONAL LIBRARY  
 OF CANADA to microfilm this thesis and to lend or sell copies  
 of the film.

The author reserves other publication rights, and  
 neither the thesis nor extensive extracts from it may be  
 printed or otherwise reproduced without the author's  
 written permission.

(Signed) *Eric K.L. Hung* .....

PERMANENT ADDRESS:

*10932-72 Ave* .....

*Edmonton Alberta* .....

.....

DATED... *June 3* ..... 19 *70*

THE UNIVERSITY OF ALBERTA

SINGLE CHANNEL N/D CALCULATION OF

(i)  $\pi N$  PARTIAL WAVES and

(ii) EFFECTS OF INELASTICITY ON  
RESONANCES

by



ERIC KAM-LING HUNG

A THESIS

SUBMITTED TO THE FACULTY OF GRADUATE STUDIES  
IN PARTIAL FULFILMENT OF THE REQUIREMENT FOR  
THE DEGREE OF DOCTOR OF PHILOSOPHY

DEPARTMENT OF PHYSICS

EDMONTON, ALBERTA

FALL, 1970

UNIVERSITY OF ALBERTA

FACULTY OF GRADUATE STUDIES

The undersigned certify that they have read, and recommend to the Faculty of Graduate Studies for acceptance, a thesis entitled SINGLE CHANNEL N/D CALCULATION OF (i)  $\pi$ N PARTIAL WAVES AND (ii) EFFECTS OF INELASTICITY ON RESONANCES, submitted by Eric Kam-Ling Hung, in partial fulfillment of the requirements for the degree of Doctor of Philosophy.

*Amkamel*  
.....  
Supervisor

*A. J. Coppi*  
.....

*Baraga*  
.....

*Douglas M. Sheppard*  
.....

*James P. Willey*  
.....  
External Examiner

Date : May 28, 1970.

## ABSTRACT

Two problems have been presented in this Thesis. The first problem in Chapter 1 is a re-analysis of the  $J \leq \frac{3}{2} \pi N$  partial waves in a single-channel N/D scheme. The new features are inclusion of (i) inelastic unitarity, and (ii) the forces generated by the exchange of a scalar  $I=0$  meson. This calculation shares the same difficulties with the previous one-channel treatments in that (a) the  $D_{13}$  resonance is absent, and (b) it is not possible to produce the nucleon as a bound state and at the same time obtain a  $P_{11}$  resonance. Apart from the  $S_{11}$ ,  $P_{11}$  and  $D_{13}$  waves, one can secure good agreement between theory and experiments in other partial waves. Chapter 2 is a model one-channel N/D calculation for studying the effect of inelasticity on position and width of a resonance.

## ACKNOWLEDGEMENT

I take great pleasure to have this opportunity to thank my supervisor, Dr. A.N. Kamal, for his constant interest and patient guidance throughout the entire course of my study at the University of Alberta.

I also wish to acknowledge financial support in the form of a Graduate Teaching and Research Assistantship from the Department of Physics, University of Alberta, and a bursary grant from the National Research Council of Canada.

## CONTENTS

	<u>Page</u>
CHAPTER ONE : A ONE CHANNEL N/D CALCULATION OF THE $\pi$ N PARTIAL WAVES INCORPORATING INELASTIC UNITARITY	1
Figure Captions	2
1. Introduction	4
2. The $J \leq \frac{3}{2}$ $\pi$ N partial waves	6
A. Results of phase shift analysis	6
B. Resonances	12
3. One-channel N/D calculation of $\pi$ N scattering	20
A. Survey	20
B. Kinematics	22
C. Interaction terms	31
D. N/D dispersion relations	39
E. Calculation and results	43
F. Conclusions	60
Appendices	61
A. Mandelstam representation of invariant amplitudes	61
B. Projection operators	66
C. An estimate of the coupling constants $g_{\sigma\pi\pi}$ and $G_{\sigma}$	68
References	70

	<u>Page</u>
CHAPTER TWO : EFFECTS OF INELASTICITY ON RESONANCES	72
Figure Captions	73
1. Introduction	75
2. Kinematics	76
3. Equations	82
4. Results and discussions	86
References	97

## CHAPTER ONE

A ONE-CHANNEL N/D CALCULATION OF THE  $\pi N$   
PARTIAL WAVES INCORPORATING INELASTIC UNITARITY



## FIGURE CAPTIONS

	<u>Page</u>
Figure 1 : Phase Shifts for $I=\frac{1}{2}$ , $J \leq \frac{3}{2}$ Partial Waves.	7
Figure 2 : Inelastic Parameters for $I=\frac{1}{2}$ , $J \leq \frac{3}{2}$ Partial Waves.	8
Figure 3 : Phase Shifts for $I=\frac{3}{2}$ , $J \leq \frac{3}{2}$ Partial Waves.	10
Figure 4 : Inelastic Parameters for $I = \frac{3}{2}$ , $J \leq \frac{3}{2}$ Partial Waves.	11
Figure 5 : Locus of $2kf$ .	13
Figure 6 : A Pure Elastic Resonance.	14
Figure 7 : Locus of $2kf$ for $R = \text{constant}$ in the neighbourhood of a resonance: (1) $R < 2$ , (2) $R > 2$ , (3) $R > 2$ with attractive back- ground, (4) $R > 2$ with repulsive background.	16
Figure 8 : Argand Diagrams for $S_{11}$ (1709 MeV), $D_{13}$ (1526 MeV), $P_{11}$ (1466 MeV), and $P_{33}$ (1236 MeV).	18
Figure 9 : Diagram for $\pi N$ Scattering.	23
Figure 10: Exchange of $\sigma, \rho$ in the $t$ -channel.	29
Figure 11: Exchange of $N, N^*$ in the $u$ -channel.	30
Figure 12: Output nucleon mass in $P_{11}$ channel for a potential generated by $\rho, N$ and $N^*$ . Elastic unitarity employed.	48
Figure 13: Output $N^*$ resonance mass in $P_{33}$ channel for various values of $G_\sigma$ . Elastic uni- tarity employed.	49

Figures 14-21 : Phase shifts for a potential generated by  $\rho$ ,  $N$  and  $N^*$ . The heavy circles are experimental results. The dash-dotted, dashed and dotted lines are results with elastic unitarity and  $WC = 18.5, 21.1$  and  $25.1$  respectively. The solid curves are results with inelastic unitarity and  $WC = 21.1$ .

50

Figures 22,23 : The solid and dash-dotted curves are results with elastic unitarity for  $G_\sigma = 12$  and  $-12$  respectively. The dashed and dotted curves are results with elastic unitarity and  $G_\sigma = 12$  and  $-12$  respectively.  $WC = 21.1$  in all four calculations.

58

## 1. INTRODUCTION

In recent years much progress has been made in our understanding of pion-nucleon scattering. Due to the rapid accumulation of experimental data and techniques in analyzing these results<sup>1-5)</sup>,  $\pi N$  partial waves are now known in considerable detail up to about 2 GeV pion laboratory energy. On the theoretical side attempts have been made to calculate these partial waves using single or multi-channel N/D dispersion relations<sup>6-15)</sup>. The advantage of using dispersion relations is that one can inject into the calculations well established principles such as analyticity, unitarity, crossing symmetry, Lorentz invariance, conservation of isotopic spin and conservation of energy-momentum. A success with theoretical models would provide us with a deeper insight into the theory of strong interactions.

In multi-channel treatments<sup>13-15)</sup>, the first channel is  $\pi N \rightarrow \pi N$ , the other channels are  $\sigma N \rightarrow \sigma N$ , etc. Inelastic reactions such as  $\pi N \rightarrow \sigma N$  arise from the coupling of the first channel to other channels. The complexity of a full calculation is enormous, but the computed two-channel results are in good agreement with those obtained by phase shift analysis of experimental data.

Single-channel N/D dispersion relations<sup>6-12)</sup> are much simpler to handle. Here the elastic channel is

$\pi N \rightarrow \pi N$ , and the coupling of this channel to other channels is described by an inelastic parameter  $\eta$ . Thus far the computed results for the  $J \leq \frac{3}{2}$  partial waves are unsatisfactory for the  $S_{11}$ ,  $P_{11}$  and  $D_{13}^\dagger$  partial waves. It is a general belief that the  $D_{13}$  wave should be solved in a multi-channel calculation. However it is not clear whether correct results for  $S_{11}$  and  $P_{11}$  can only be obtained by using a multi-channel dispersion relation, or that the 'potentials' used were inadequate<sup>12)</sup>. In this present work a reanalysis of the  $J \leq \frac{3}{2}$  partial waves is made by using a more complicated potential. It is hoped that the results would shed some light on the difficulties encountered.

---

<sup>†</sup> The convention  $l_{2I,2J}$  is used to denote partial waves with isospin  $I$ , total angular momentum  $J$  and orbital angular momentum  $l$ .

## 2. THE $J \leq \frac{3}{2}$ $\pi N$ PARTIAL WAVES

### A. Results of Phase Shift Analysis

In recent years partial wave analysis of  $\pi N$  scattering has been carried out at Saclay<sup>2)</sup>, CERN<sup>3)</sup> and Berkeley<sup>4)</sup>. The most recent results from these centres have been summarized by Lovelace in Reference 5 (a review of older analyses is given by Donnachie in Reference 1). Despite the use of different data and methods, the results of different groups are consistent with one another for large amplitudes and strong resonances. In the following the main features of the  $J \leq \frac{3}{2}$  partial waves have been summarized.

Partial wave amplitudes, with  $I, J, \ell$  suppressed, are defined by

$$f(W) = \frac{\eta(W)e^{2i\delta(W)} - 1}{2ik}, \quad (2.1)$$

where  $W$  is the sum of nucleon energy  $E$  and pion energy  $\omega$ ,  $\eta$  is the inelastic parameter, and  $\delta$  is the real part of phase shift (since no confusion arises,  $\delta$  will henceforth be referred to as phase shift). The meaning of resonances and its detection is given in Section 2B.

$I = \frac{1}{2}$  Scattering (Figures 1 and 2)

$S_{11}$  The phase shift  $\delta$  increases from zero to about  $10^\circ$  at 50 MeV pion laboratory energy. It remains more or less constant at this value up to 300 MeV and

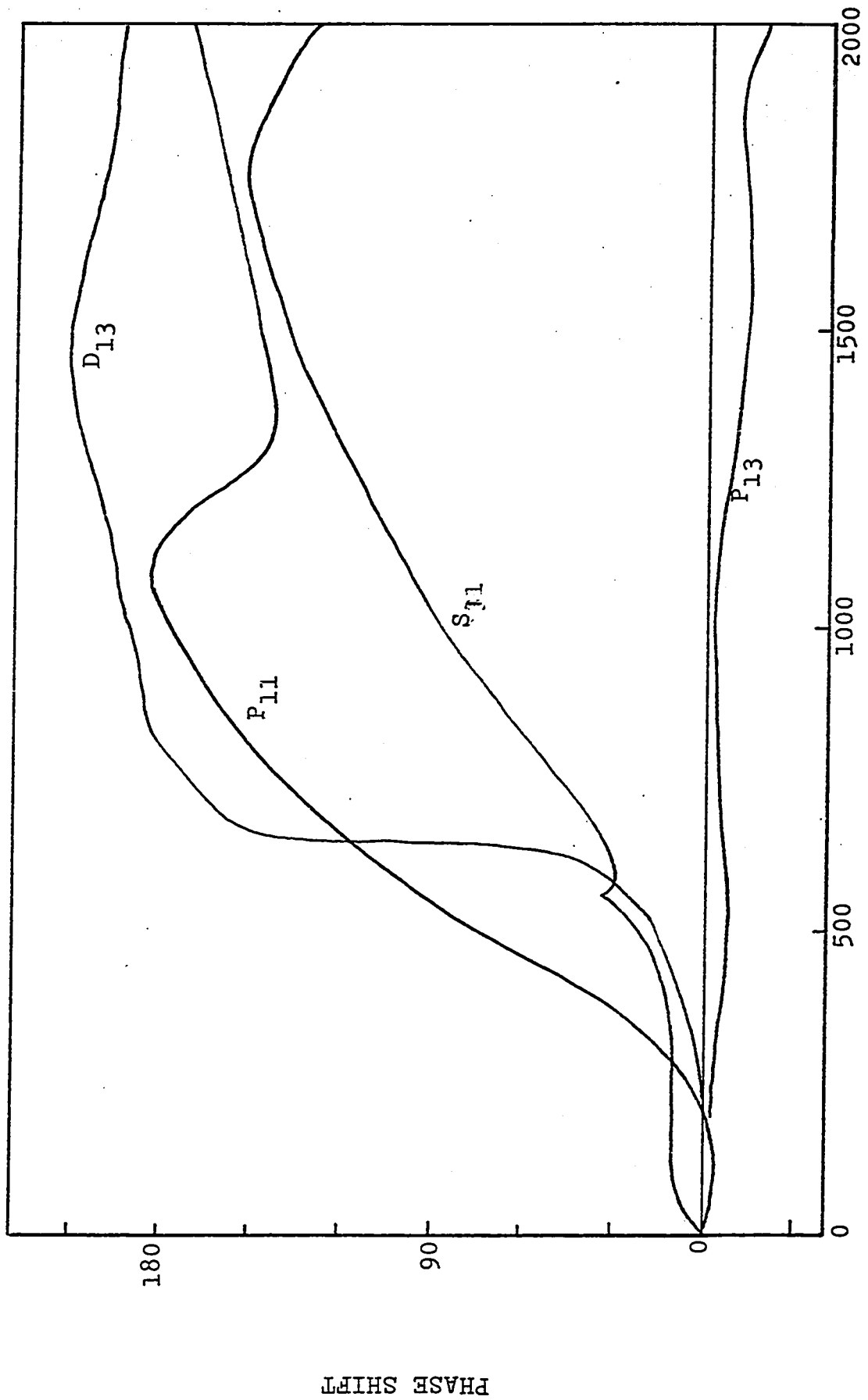


Figure 1 PION LABORATORY ENERGY (MeV)

PHASE SHIFT

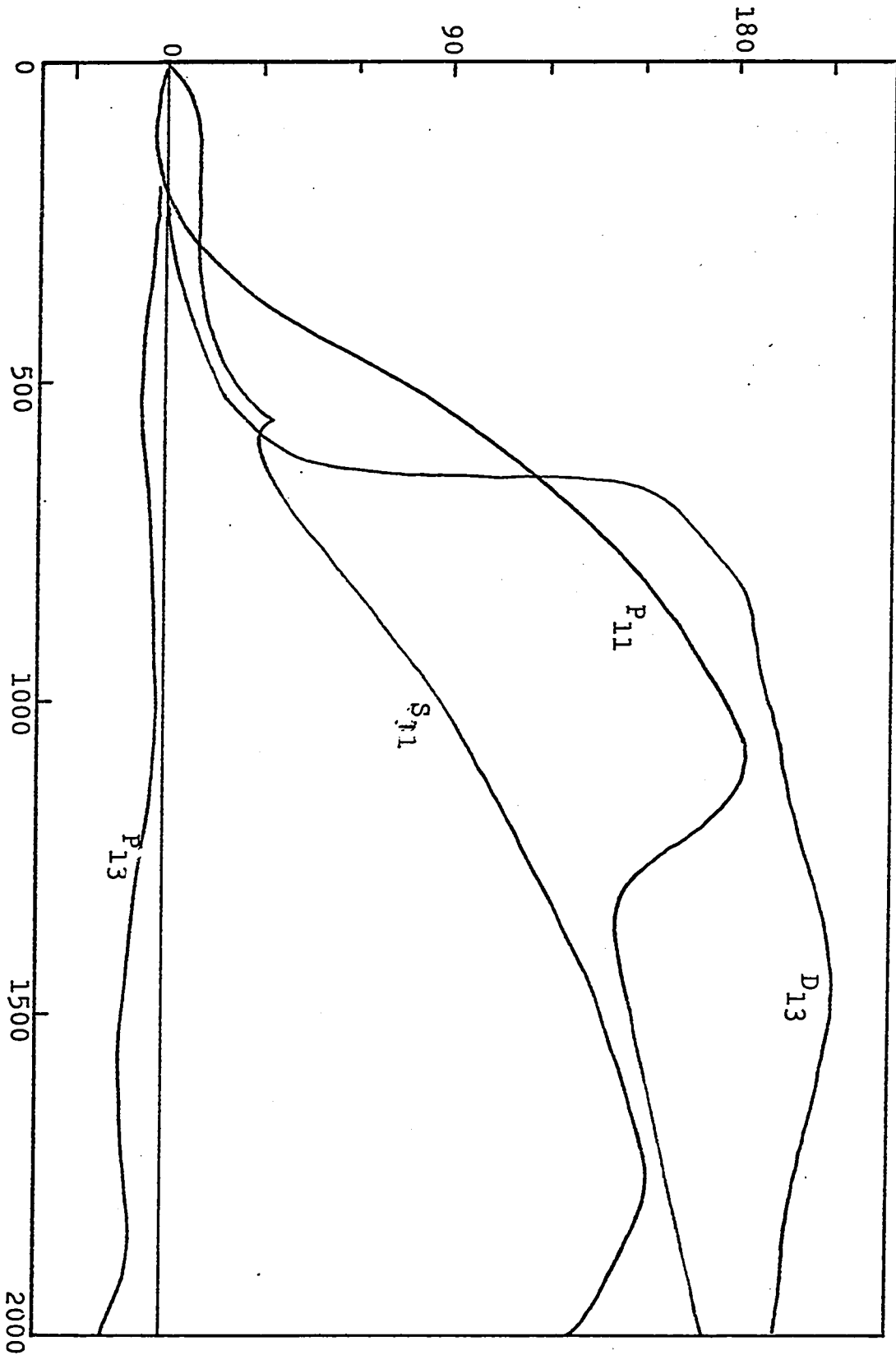
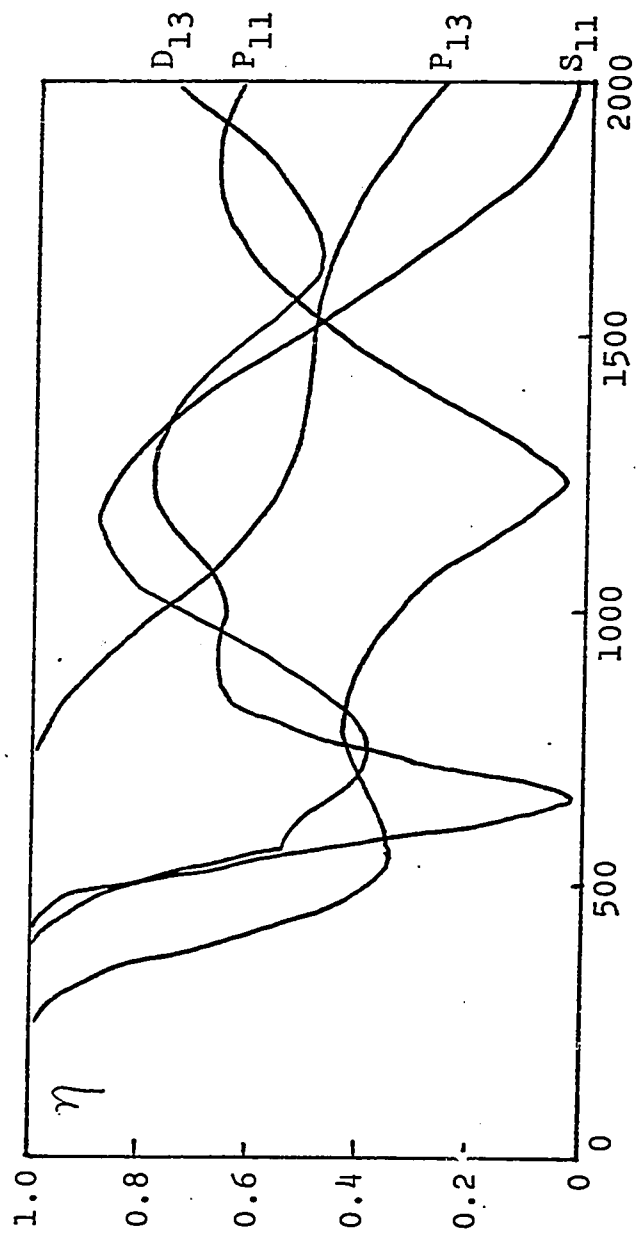


Figure 1

PION LABORATORY ENERGY (MeV)



INELASTICITY PARAMETER

PION LABORATORY ENERGY (MeV)

Figure 2



then rises up  $150^\circ$  at 1800 MeV where it starts falling rapidly. The inelastic parameter  $\eta$  in Figure 2 decreases from unity (corresponding to elastic scattering) at 400 MeV to  $\eta \approx 0.4$  at 700 MeV, rises up to  $\eta \approx 0.9$  at 1100 MeV and then decreases rapidly to almost zero (corresponding to very inelastic scattering) at 2 GeV. The rise of  $\delta$  through  $90^\circ$  at 900 MeV can be interpreted in terms of an  $S_{11}$  resonance with mass 1709 MeV.

$P_{11}$  The phase shift is small and negative below 200 MeV and rises through  $90^\circ$  at 600 MeV to give a  $P_{11}$  resonance with mass 1466 MeV. After passing through  $180^\circ$  at 1100 MeV it falls down rapidly to  $120^\circ$  and then rises up more gradually. Figure 2 shows that  $\eta < 0.4$  in the energy range 500 to 1500 MeV, so that a considerable fraction of the force producing the  $P_{11}$  resonance arises from inelastic channels.

$P_{13}$  The phase shift is small and negative ( $-25^\circ < \delta \leq 0$ ) up to 2 GeV. The inelastic parameter  $\eta$  is close to unity up to 700 MeV, above which it decreases gradually to  $\eta \approx 0.3$  at 2 GeV.

$D_{13}$  The phase shift rises steeply through  $90^\circ$  at 600 MeV, (centre of mass energy 1526 MeV) accompanied by a deep minimum in  $\eta$  ( $\eta \approx 0$ ) at this energy. Above 800 MeV  $\delta$  stays around  $160^\circ$  with  $\eta \approx 0.7$ .

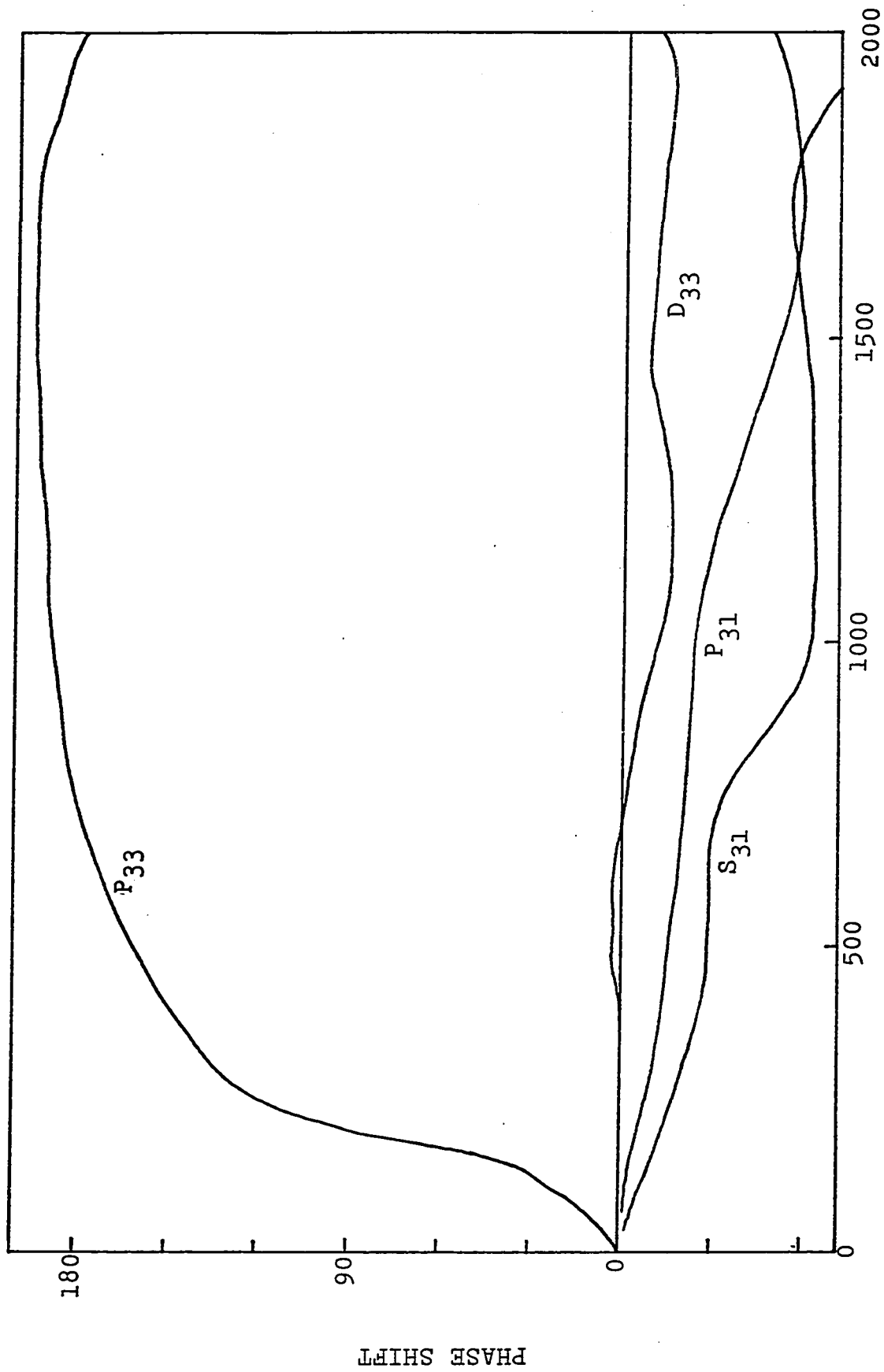


Figure 3 PION LABORATORY ENERGY (MeV)

10

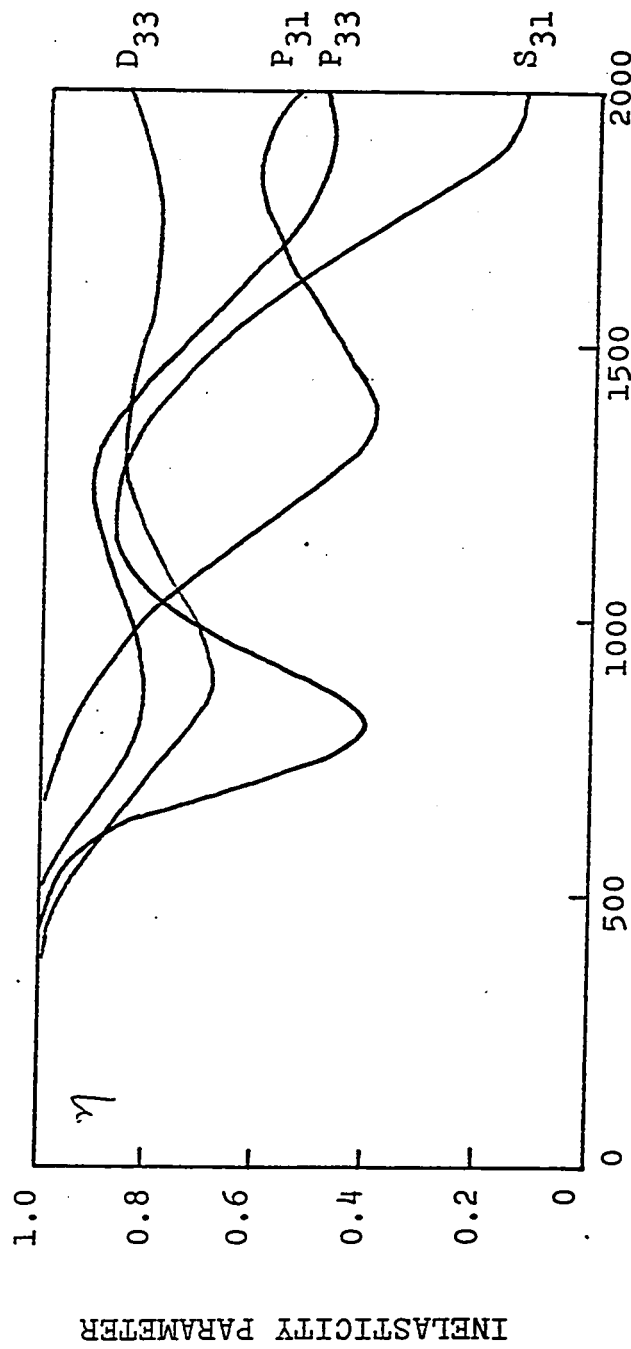


Figure 4  
PION LABORATORY ENERGY (MeV)

$I = \frac{3}{2}$  Scattering (Figures 3 and 4)

$S_{31}$  There are dips in  $\eta$  at 800 MeV ( $\eta \approx 0.4$ ) and 1900 MeV ( $\eta \approx 0.2$ ) accompanied by rapid drops in the phase shift, which is negative at all energies.

$P_{31}$  This phase shift decreases more or less gradually from zero to  $-60^\circ$  at 2 GeV. It is elastic below 600 MeV. Above this energy  $\eta$  decreases slowly to 0.5 at 2 GeV. There is a shallow minimum ( $\eta \approx 0.4$ ) at 1400 MeV.

$P_{33}$  This partial wave possesses the well known  $N^*$  resonance,  $P_{33}$  (1236 MeV), at 200 MeV, where the phase shift rises through  $90^\circ$  to reach  $170^\circ$  at 600 MeV and remains more or less constant there. The inelastic parameter is very close to unity below 500 MeV and decreases gradually to  $\eta \approx 0.5$  at 2 GeV. There are shallow minima at 900 MeV ( $\eta \approx 0.8$ ) and 1900 MeV ( $\eta \approx 0.5$ ).

$D_{33}$  This partial wave has small phase shifts ( $|\delta| < 15^\circ$ ) and little inelasticity ( $\eta > 0.7$ ) up to 2 GeV.

## B. Resonances

One of the most important results in partial wave analysis is the discovery of resonances in the  $\pi N$  system. A resonance is defined as a pole of the S-matrix on the unphysical sheet. However since the data exist for real

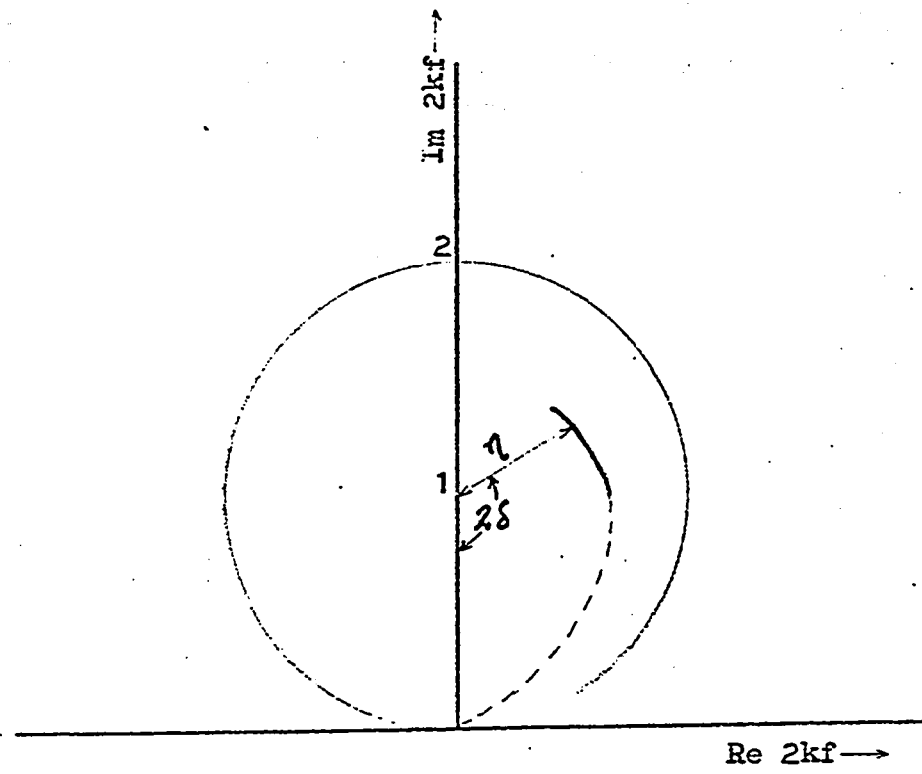


Figure 5

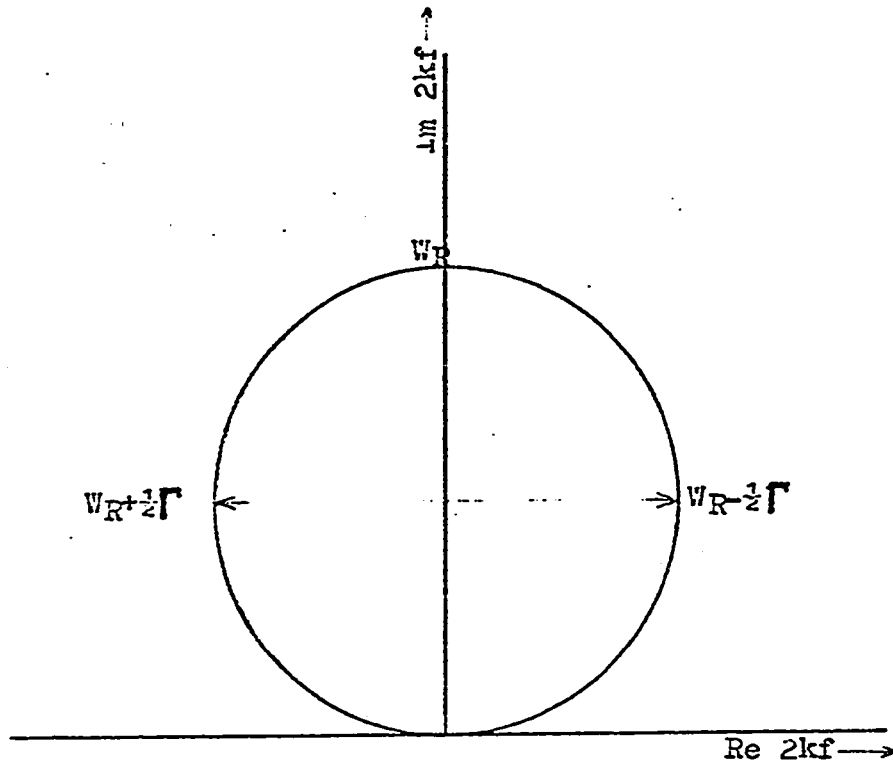


Figure 6

energies alone, some resonance recognition criteria have to be employed on the real energy axis. The techniques currently favoured to detect the presence of resonances in a given partial wave is to plot the quantity  $2kf$  on an Argand diagram (Figure 5).

For a pure elastic resonance (Figure 6)  $2kf$  traces out an arc of a circle with centre  $i$  in a counterclockwise direction. The resonance energy  $W_R$  appears at the top of the circle, and the width  $\Gamma$  is given by the difference of energies at the horizontal diameter as shown.

In general inelastic effects and non-resonant backgrounds are present, and the locus of  $2kf$  becomes a smaller, distorted circle inside the unit circle (Figure 7). Their effects will be discussed as follows:

(a) Inelasticity with negligible non-resonant background

The locus of  $2kf$  at any given energy is an arc of a circle with radius  $\frac{1}{R}$  and centre  $\frac{i}{R}$ , where

$$R = \frac{\text{Im } f}{k|f|^2} \geq 1 \quad (2.2)$$

is the ratio of total cross-section to elastic cross-section. For  $R < 2$  everywhere (Curve 1 in Figure 7) the locus passes above the centre of the unit circle, and  $\delta$  rises through  $90^\circ$  at the resonance in the same manner as the pure elastic case. This is called a

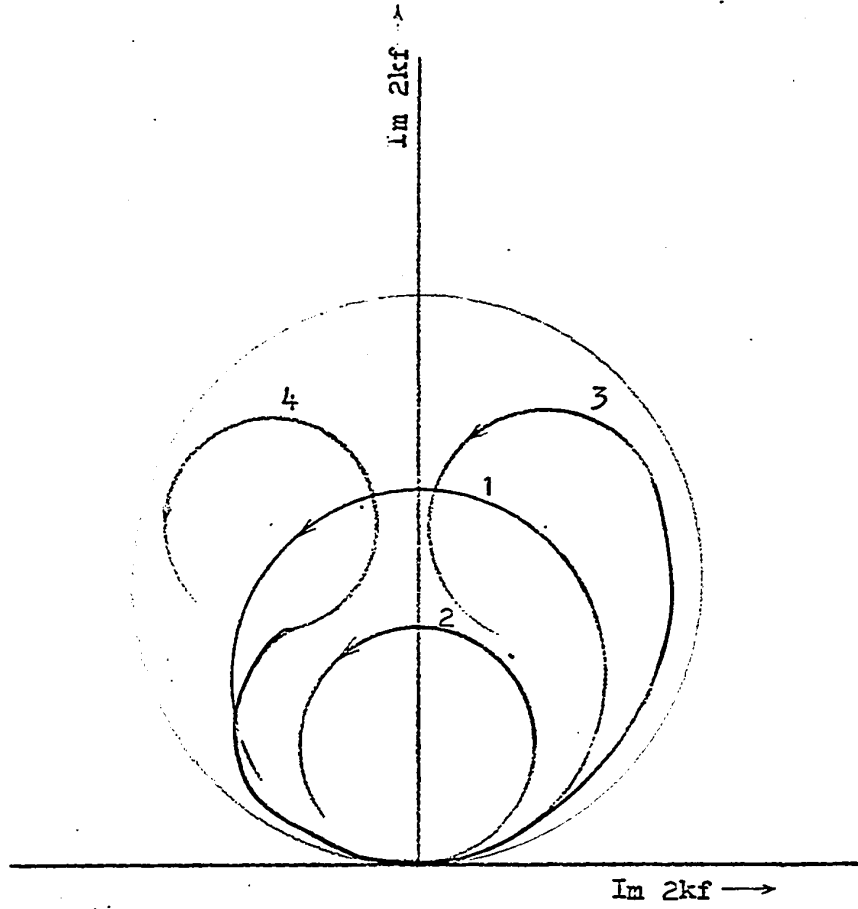


Figure 7



quasi-elastic resonance. For  $R > 2$  everywhere (Curve 2) the locus passes below the centre of the unit circle. This is called an inelastic resonance because  $\delta$  rises to a maximum value which is less than  $45^\circ$ , decreases through  $0^\circ$  at the resonance to reach a minimum which is greater than  $-45^\circ$  and then rises again. In both cases  $\eta$  is minimum and  $|d(2kf)/dW|$  is maximum at the resonance.

(b) Inelasticity with strong non-resonant backgrounds

One way to include this background is to assume that the resonance and the background multiply in the S-matrix, so that each is unitary separately. This gives  $\delta = \delta_R + \delta_B$ ,  $\eta = \eta_R \eta_B$ , where the subscripts R and B denote the resonance and background contributions respectively. The net result is to shift the locus for  $2kf$  to the right (left) if the background is attractive (repulsive). Curves 3 and 4 in Figure 7 are examples with attractive and repulsive backgrounds respectively. Since  $\delta_B$  also contributes to the phase shift  $\delta$ , the resonance position is not determined either by the condition  $\delta$  rising through  $90^\circ$ , or that  $\text{Im } f$  is maximum. It is normally chosen as the energy with  $\eta$  minimum or  $|d(2kf)/dW|$  maximum.

In actual  $\pi N$  phase shift analysis, anything which looped counterclockwise was considered a resonance [Figure 8 is an example for  $S_{11}$  (1709 MeV),  $P_{11}$  (1466 MeV)]

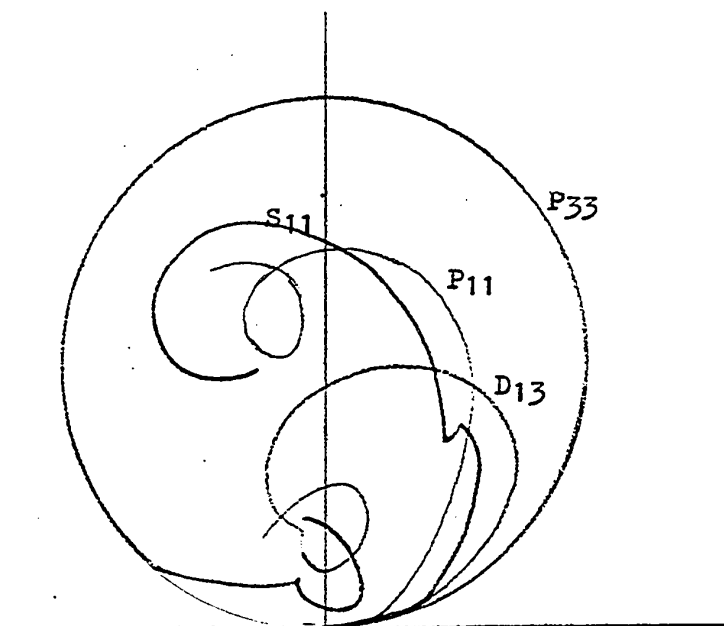


Figure 8

$D_{13}$  (1526 MeV) and  $P_{33}$  (1236 MeV) in the CERN set].  
Sets of resonance parameters have been obtained with  
 $\eta$  minimum (CERN)<sup>2)</sup>,  $|d(2kf)/dW|$  maximum (Saclay)<sup>3)</sup>  
and  $\text{Im}f$  maximum (Saclay also).

### 3. ONE-CHANNEL N/D CALCULATION OF $\pi$ N SCATTERING

#### A. Survey

The problem of calculating the  $\pi$ N scattering amplitude by solving the partial wave dispersion relation using the one-channel N/D method has been discussed by various authors in the past<sup>6-12)</sup>. Of these authors Ball and Wong<sup>9)</sup> were mainly interested in seeing if, in a relativistic treatment with a 'potential' generated by exchange of  $\rho$ , N and N\* (1236 MeV), the N\* resonance in P<sub>33</sub> channel could be produced simultaneously with a dynamically bound nucleon in P<sub>11</sub> channel. By using a single cut off on the N/D equations, they succeeded in producing the N\* at its correct position together with a loosely bound nucleon in P<sub>11</sub>. Other phase shifts for  $J \leq \frac{3}{2}$  were also calculated, it being found that with the exception of S<sub>11</sub> and P<sub>11</sub> waves, the low energy results were in qualitative agreement with experiments<sup>1-5)</sup>.

Choudhury et al.<sup>11)</sup> essentially repeated the calculations of Ball and Wong with the inclusion of isoscalar mesons in the t-channel without any improvement on the above mentioned results.

Coulter and Shaw<sup>10,12)</sup> studied the same problem with both elastic and inelastic unitarity. In their first calculation<sup>10)</sup> using a potential generated by exchange of  $\rho$ , N and N\*, they found that with the excep-

tion of  $S_{31}$  and  $P_{13}$  waves, better results were obtained with the inclusion of inelastic effects up to 700 MeV pion laboratory energy. However the  $S_{11}$  and  $P_{11}$  waves continued to disagree with experiments unless a nucleon pole with the correct residue and position was included in the s-channel, in which case the two coupled waves agreed with experiments up to 600 MeV.

With the discovery of new resonances in  $S_{11}$ ,  $P_{11}$ ,  $S_{31}$  and  $D_{31}$  channels, they carried out a second calculation<sup>13)</sup> with these particles included in the u-channel continua. Their results showed that: (1) Compared with exchange of N and  $N^*$  the contributions to the s-channel unphysical cut from the  $S_{11}$ ,  $P_{11}$  and  $S_{31}$  resonances were small. (2) The  $D_{13}$  contribution was divergent at large s; the effect of including this resonance in the u-channel was to make the results worse. (3) The detailed shape of the  $N^*$  resonance reduced its contribution to the exchange potential by 25% compared with the narrow width approximation. The general conclusion on the coupled  $S_{11}$  and  $P_{11}$  wave was that, in a simple one-channel N/D treatment which forced the nucleon to appear as a dynamical bound state, the computed phase shifts disagreed with experiments. It was not clear whether a more complicated potential was necessary, or that a multi-channel calculation had to be performed.

The question whether the nucleon can be obtained as a bound state in a single-channel calculation has been studied by Rothleitner and Stech<sup>16)</sup>, with the conclusion that for the nucleon to be a bound state, the  $P_{11}$  phase must have a negative sign at the inelastic threshold; a positive phase excludes the bound state picture but allows a  $P_{11}$  resonance to occur.

From the preceding discussions it would seem that a one-channel N/D calculation is not capable of producing satisfactory  $S_{11}$  and  $P_{11}$  phase shift behaviour. In this present work the problem has been reanalysed with the inclusion of a scalar  $I = 0$  meson (called  $\sigma$ -meson) in the potential. Inelasticity has also been included. The results obtained indicate that discrepancies between theory and experiment persist for the coupled  $S_{11}$  and  $P_{11}$  phase shifts.

## B. Kinematics

This section contains a brief summary of the kinematics in  $\pi N$  scattering. A more detailed discussion can be found in many books<sup>†</sup>. We would work in the centre of mass system with a metric  $g_{00} = 1$ ,  $g_{11} = g_{22} = g_{33} = -1$ ,

---

<sup>†</sup> See, for example, M. Jacob and G.F. Chew: Strong Interaction Physics (W.A. Benjamin, Inc., New York, 1964).

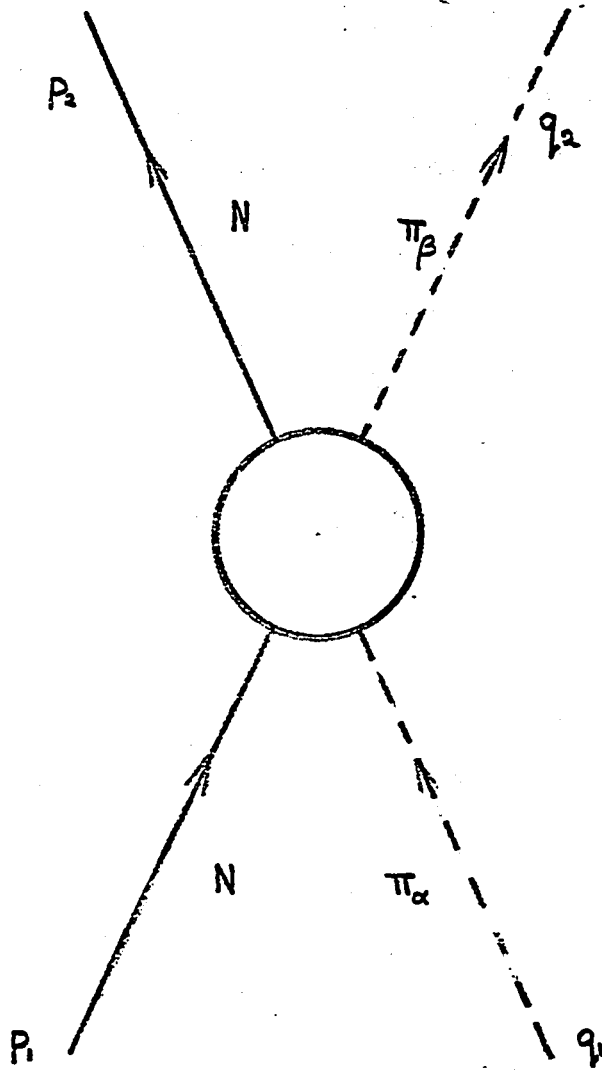


Figure 9

and units  $c=\hbar=\mu=1$ , where  $\mu$  is the pion mass.

Referring to Figure 9 for  $\pi N$  scattering, the kinematical invariants are

$$\left. \begin{aligned} s &= (p_1 + q_1)^2 = W^2 = (E + \omega)^2, \\ t &= (p_1 - p_2)^2 = -2k^2(1 - x), \\ u &= (p_1 - q_2)^2 = 2m^2 + 2 - s - t, \end{aligned} \right\} \quad (3.1)$$

where  $p_1, p_2$  are the initial and final 4-momenta of the nucleon with mass  $m$ ,  $q_1, \alpha$  and  $q_2, \beta$  are the initial and final 4-momenta and isospins of the pion with mass  $\mu$ , and  $x$  is the cosine of the scattering angle  $\theta$ . Suppress-isospin indices, the S-matrix for elastic scattering between the final state  $f$  and initial state  $i$  can be written as

$$\begin{aligned} S_{fi} &= \delta_{fi} - i(2\pi)^4 \delta^4(p_1 + q_1 - p_2 - q_2) \frac{2m}{(2\pi)^6 \sqrt{2E_1 2E_2, 2\omega_1 2\omega_2}} \\ &\times \bar{u}_f(p_2) T(s, t, u) u_i(p_1). \end{aligned} \quad (3.2)$$

The amplitude  $T(s, t, u)$  is a  $4 \times 4$  matrix between spinors  $u_f(p_2)$  and  $u_i(p_1)$  with the most general form

$$T(s, t, u) = A(s, t, u) + \frac{q_1 + q_2}{2} B(s, t, u) \quad (3.3)$$



where  $A(s,t,u)$  and  $B(s,t,u)$  are invariants containing all of the dynamics of  $\pi N$  interaction (Appendix A), and  $\not{q} = \gamma^\mu q_\mu$

$$\left. \begin{aligned} \gamma^0 &= \begin{pmatrix} I & 0 \\ 0 & -I \end{pmatrix}, \quad \gamma^k = \begin{pmatrix} 0 & \sigma^k \\ -\sigma^k & 0 \end{pmatrix}, \quad \sigma^1 = \begin{pmatrix} 0 & 1 \\ 1 & 0 \end{pmatrix}, \\ \sigma^2 &= \begin{pmatrix} 0 & -i \\ i & 0 \end{pmatrix}, \quad \sigma^3 = \begin{pmatrix} 1 & 0 \\ 0 & -1 \end{pmatrix}. \end{aligned} \right\} \quad (3.4)$$

This T matrix can be related to the  $2 \times 2$  matrix

$$f \equiv f_1 + \frac{(\underline{\sigma} \cdot \underline{q}_1)(\underline{\sigma} \cdot \underline{q}_2)}{k^2} f_2 \quad (3.5)$$

between 2-component spinors  $\chi_f, \chi_i$  by

$$\begin{pmatrix} f_1 \\ f_2 \end{pmatrix} = \frac{1}{4\pi} \alpha \begin{pmatrix} A \\ B \end{pmatrix}, \quad (3.6)$$

where

$$\alpha = \frac{1}{2W} \begin{pmatrix} E + m & (W-m)(E+m) \\ -(E-m) & (W+m)(E-m) \end{pmatrix}. \quad (3.7)$$

Conversely

$$\begin{pmatrix} A \\ B \end{pmatrix} = 4\pi \begin{pmatrix} \frac{W+m}{E+m} & -\frac{W-m}{E-m} \\ \frac{1}{E+m} & \frac{1}{E-m} \end{pmatrix} \begin{pmatrix} f_1 \\ f_2 \end{pmatrix}. \quad (3.8)$$

In terms of T and f, the differential cross-section is given by

$$\frac{d\sigma}{d\Omega} = \left| \frac{2m}{8\pi W} \bar{u}_f(\underline{p}_2)^T u_i(\underline{p}_1) \right|^2 = |X_f^\dagger X_i|^2. \quad (3.9)$$

The amplitudes  $f_1$  and  $f_2$  are related to partial wave amplitudes by

$$f_1(W) = \sum_{\ell} [f_{\ell+}(W) P'_{\ell+1}(x) - f_{\ell-}(W) P'_{\ell-1}(x)], \quad (3.10)$$

$$f_2(W) = \sum_{\ell} [f_{\ell-}(W) - f_{\ell+}(W)] P'_{\ell}(x),$$

with the inverse relation

$$f_{\ell\pm}(W) = \frac{1}{2} \int_{-1}^1 dx [f_1(W) P_{\ell}(x) + f_2(W) P_{\ell\pm 1}(x)]. \quad (3.11)$$

The convention is to write  $\ell\pm$  for  $J = \ell \pm \frac{1}{2}$ , since the nucleon spin can combine with a given orbital angular momentum  $\ell$  to produce two different total angular momentum states.

The phase shift representation for the partial waves is

$$f_{\ell\pm}(W) = \frac{\eta_{\ell\pm}(W) e^{2i\delta_{\ell\pm}(W)} - 1}{2ik} \quad (2.1'), (3.12)$$

where  $\delta_{\ell\pm}(W)$  is the real part of phase shift, and  $\eta_{\ell\pm}(W)$  is the inelastic parameter.

Defining

$$[A_{\ell}(s,t,u), B_{\ell}(s,t,u)] = \int_{-1}^1 [A(s,t,u), B(s,t,u)] P_{\ell}(x) dx, \quad (3.13)$$

one can write

$$f_{\ell\pm}(W) = \frac{1}{8\pi} \{ \alpha_{11} A_{\ell} + \alpha_{12} B_{\ell} + \alpha_{21} A_{\ell\pm 1} + \alpha_{22} B_{\ell\pm 1} \}. \quad (3.14)$$

Noting that

$$\left. \begin{aligned} \alpha^*(W) &= \alpha(W^*) \quad , \\ \alpha_{11}(-W) &= -\alpha_{21}(W) \quad , \\ \alpha_{12}(-W) &= -\alpha_{22}(W) \end{aligned} \right\} \quad (3.15)$$

one gets the famous MacDowell's symmetry relation<sup>6,17)</sup>

$$f_{\ell\pm}(-W) = -f_{(\ell\pm 1)\mp}(W) \quad , \quad (3.16)$$

which can be combined with the reality condition

$$f_{\ell\pm}(z^*) = f_{\ell\pm}^*(z) \quad (3.17)$$

to give

$$\left. \begin{aligned} \eta_{\ell+}(-W + i\varepsilon) &= \eta_{(\ell+1)-}(W + i\varepsilon), \quad W > WI, \\ \delta_{\ell+}(-W + i\varepsilon) &= -\delta_{(\ell+1)-}(W + i\varepsilon), \quad W > (m+1) \end{aligned} \right\} \quad (3.18)$$

and

where  $WI$  is the inelastic threshold.

Equations (3.16) and (3.17) show that, for a given total angular momentum  $J$  of the  $\pi N$  system, the two orbital angular momentum states  $\ell = J \pm \frac{1}{2}$  are related to each other by

$$f_{(\ell+1)-}(W + i\epsilon) = -f_{\ell+}(-W - i\epsilon) = -f_{\ell+}^*(-W + i\epsilon), \quad (3.19)$$

so that one can solve for  $f_{\ell+}(W + i\epsilon)$  in the positive energy region and extract the results for  $f_{(\ell+1)-}(W + i\epsilon)$  from the negative energy region. It also states that for a given  $J$  the physical amplitude for one orbital angular momentum state should form part of the driving force for the physical amplitude of the other orbital angular momentum state. Thus, the two orbital momentum states are coupled with each other and should be solved simultaneously.

The following relations are found useful and can be verified easily,

$$\begin{aligned} E &= \frac{s + m^2 - 1}{2W}, & , \\ \omega &= \frac{s - m^2 + 1}{2W}, & , \\ E \pm m &= \frac{(W \pm m)^2 - 1}{2W}, & , \\ k^2 &= (E^2 - m^2) = \frac{1}{4} \left\{ s - 2(m^2 + 1) + \frac{(m^2 - 1)^2}{s} \right\}, \\ x &= \frac{t + 2k^2}{2k^2} = \frac{1}{2(E^2 - m^2)} \left\{ m^2 + 1 - \frac{s}{2} u + \frac{(m^2 - 1)^2}{2s} \right\}. \end{aligned} \quad (3.20)$$

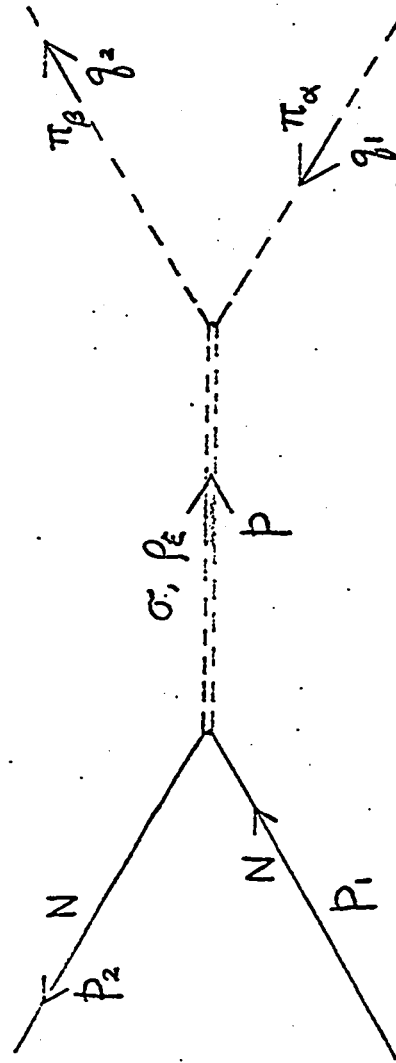


Figure 10

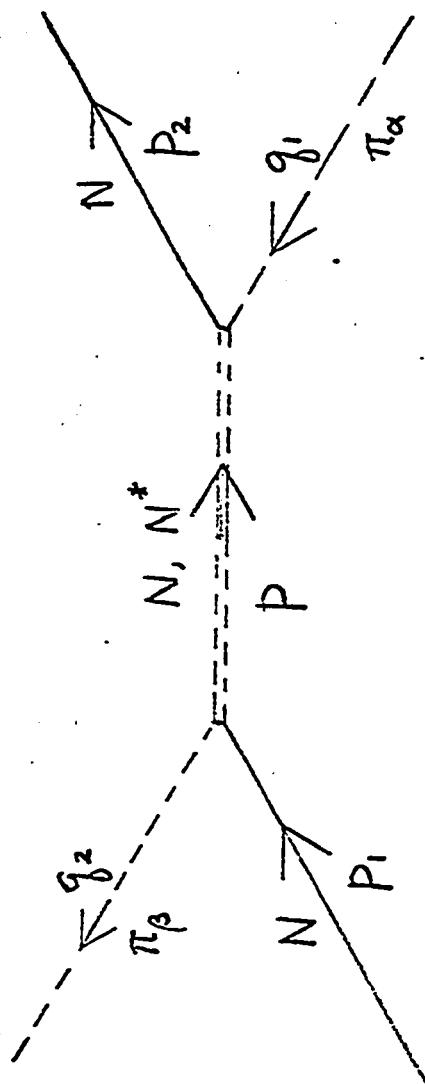


Figure 11

### C. Interaction Terms

It is possible to discuss  $\pi N$  scattering by considering the partial wave amplitude  $f_{\ell\pm}$ . All of the dynamics are contained in the invariants A and B. Due to the lack of detailed information on pion-nucleon forces, approximate values for A and B will be obtained with exchange of  $\sigma$ ,  $\rho$ , N and  $N^*$  in the crossed channels as shown in Figures 10 and 11. These are the longest range forces known to exist; the remaining shorter range forces will be taken into account by using a cut-off parameter in Section 3E. The contributions from  $\sigma$ ,  $\rho$  and N are computed using Feynman diagrams<sup>†</sup>, but those from the  $N^*$  resonance will be obtained with dispersion relations. A discussion of projection operators used in this section is given in Appendix B.

$\sigma$ -exchange (I=0, J=0)

This is a hypothetical particle used to study the effect of strong attractive force found to exist between two pions. While direct evidence for its existence is not yet established, there are indications<sup>11, 18-21)</sup> that it has a mass 500-900 MeV and width 100-450 MeV. In the present calculations the following values will be used

---

<sup>†</sup> The convention is the same as the book by S.S. Schweber, H.A. Bethe and F. de Hoffmann: Mesons and Fields, Volume I (Harper and Row, Publishers, Inc., New York, 1954).

$$\begin{aligned}
 m_\sigma &= 4.0 \quad (560 \text{ MeV}) \quad , \\
 G_\sigma &= \frac{g_{\sigma NN} \bar{g}_{\sigma\pi\pi}}{4\pi} = \pm 12 \quad .
 \end{aligned}
 \quad \left. \vphantom{\begin{aligned} m_\sigma \\ G_\sigma \end{aligned}} \right\} \quad (3.21)$$

An estimate for the coupling constants  $g_{\sigma NN}$ ,  $\bar{g}_{\sigma\pi\pi}$  will be given in Appendix C.

With reference to Figure 10, let  $\psi(x)$ ,  $\sigma(x)$  and  $\phi_\alpha(x)$  be the wave functions for the nucleon,  $\sigma$ -meson and pion respectively. The matrix element computed from an interaction Hamiltonian density

$$\mathcal{H}_I(x) = g_{\sigma NN} \bar{\psi}\psi\sigma + g_{\sigma\pi\pi} \underline{\phi} \cdot \underline{\phi}\sigma \quad ,$$

meson propagator

$$\frac{i}{(2\pi)^4} \frac{1}{p^2 - m_\sigma^2} \quad ,$$

and vertex functions

$$g_{\sigma NN} (2\pi)^4 \delta^4(p_1 - p_2 - p) \quad ,$$

$$2g_{\sigma\pi\pi} (2\pi)^4 \delta^4(q_2 - q_1 - p) \delta_{\beta\alpha} \quad ,$$

where  $g_{\sigma NN}$ ,  $\bar{g}_{\sigma\pi\pi}$  are coupling constants, is given by

$$\begin{aligned}
 S_{fi} &= (-i)^2 \int d^4p \left\{ \frac{1}{(2\pi)^{3/2}} \sqrt{\frac{m}{E(p_2)}} \bar{u}_f(p_2) \right\} \{ g_{\sigma NN} (2\pi)^4 \delta^4(p_1 - p_2 - p) \} \\
 &\times \left\{ \frac{1}{(2\pi)^{3/2}} \sqrt{\frac{m}{E(p_1)}} u_i(p_1) \right\} \left\{ \frac{i}{(2\pi)^4} \frac{1}{p^2 - m_\sigma^2} \right\} \left\{ \frac{1}{(2\pi)^{3/2} \sqrt{2\omega_2}} \right\}
 \end{aligned}$$



$$\begin{aligned}
& \times \{2g_{\sigma\pi\pi} (2\pi)^4 \delta^4(q_2 - q_1 - p) \delta_{\beta\alpha}\} \left\{ \frac{1}{(2\pi)^{3/2} \sqrt{2\omega_1}} \right\} \\
& = -i(2\pi)^4 \delta^4(p_1 + q_1 - p_2 - q_2) \left\{ \frac{2m}{(2\pi)^6 \sqrt{2E(p_1)2E(p_2)2\omega_1 2\omega_2}} \right\} \\
& \times \bar{u}_f(p_2) \{2g_{\sigma NN} g_{\sigma\pi\pi} \frac{\delta_{\beta\alpha}}{t - m_\sigma^2}\} u_i(p_1) .
\end{aligned}$$

Using Equations (B9), (3.2) and (3.3), one gets<sup>†</sup>

$$\left. \begin{aligned}
A\left(\frac{1}{2}; \frac{3}{2}\right) (s, t, u) &= (1; 1) \frac{2g_{\sigma NN} g_{\sigma\pi\pi}}{m_\sigma^2 - t} , \\
B\left(\frac{1}{2}; \frac{3}{2}\right) (s, t, u) &= 0 .
\end{aligned} \right\} \quad (3.22)$$

$\rho$ -meson exchange ( $I=1, J=1$ )

Here

$$\begin{aligned}
\mathcal{H}_I = & \{G_e - G_m\} \bar{\psi} \gamma_\mu \underline{I} \psi \cdot \underline{\rho}^\mu - i \frac{G_m}{2m} \{ \partial_\mu \bar{\psi} \underline{I} \psi - \\
& \bar{\psi} \underline{I} \partial_\mu \psi \} \cdot \underline{\rho}^\mu + \frac{1}{2} G_{\rho\pi\pi} \underline{\rho}^\mu \cdot (\underline{\phi}_\Lambda \partial_\mu \underline{\phi} - \partial_\mu \underline{\phi}_\Lambda \underline{\phi})
\end{aligned}$$

where  $G_e$  is a measure of the coupling between the charged  $\rho$ -meson field  $\underline{\rho}^\mu(x)$  and the electromagnetic field  $\bar{\psi} \gamma_\mu \psi$  due to the nucleon, and  $G_m$  measures the coupling between the electromagnetic field and the 'electric and magnetic

<sup>†</sup>

The convention ( $I=\frac{1}{2}; I=\frac{3}{2}$ ) for isospin index is used.

moments' of the  $\rho$ -meson. The  $\rho$ -meson propagator is

$$-\frac{i}{(2\pi)^4} \frac{1}{p^2 - m_\rho^2} \{g^{\mu\nu} - \frac{p^\mu p^\nu}{m_\rho^2}\}$$

and the vertex functions are

$$(2\pi)^4 \delta^4(p_1 - p_2 - p) \{ (G_e - G_m) \gamma_\mu + \frac{G_m}{2m} (p_1 + p_2)_\mu \} \tau_\xi,$$

$$(2\pi)^4 \delta^4(q_2 - q_1 - p) \{ -i \epsilon_{\alpha\beta\xi} G_{\rho\pi\pi} (q_1 + q_2)_\mu \},$$

giving

$$S_{f1} = -i(2\pi)^4 \delta^4(p_1 + q_1 - p_2 - q_2) \left\{ \frac{2m}{(2\pi)^6 \sqrt{2E(p_1)2E(p_2)2\omega_1 2\omega_2}} \right\} \times \\ \bar{u}_f(p_2) \left\{ \frac{i \epsilon_{\alpha\beta\xi} \tau_\xi G_{\rho\pi\pi}}{t - m_\rho^2} \left[ \frac{G_m}{2m} (p_1 + p_2)_\mu (q_1 + q_2)_\mu + 2(G_e - G_m) \frac{q_1 + q_2}{2} \right] \right\} u_i(p_1).$$

Using equations (B10), (3.2), (3.3) and

$$(p_1 + p_2)(q_1 + q_2) = s - u = 2s + t - 2m^2 - 2,$$

one has

$$\left. \begin{aligned} A\left(\frac{1}{2}; \frac{3}{2}\right) &= (2; -1)(6\pi\gamma_2) \frac{2s+t-2m^2-2}{m_\rho^2 - t} \\ B\left(\frac{1}{2}; \frac{3}{2}\right) &= (2; -1)(-12\pi) \frac{\gamma_1 + 2m\gamma_2}{m_\rho^2 - t} \end{aligned} \right\} \quad (3.23)$$

where

$$\left. \begin{aligned} 6\pi\gamma_1 &= -G_e G_{\rho\pi\pi} \\ 6\pi\gamma_2 &= \frac{G_m G_{\rho\pi\pi}}{2m} \end{aligned} \right\} \quad (3.24)$$

The mass of the  $\rho$ -meson is given by

$$m_\rho = 5.4 \quad (769 \text{ MeV}) \quad , \quad (3.25)$$

and the constants  $\gamma_1, \gamma_2$  has been estimated<sup>9,10,22</sup> to have the approximate values

$$\left. \begin{aligned} \gamma_1 &= -0.84 \quad , \\ \gamma_2 &= 0.27 \gamma_1 \quad . \end{aligned} \right\} \quad (3.26)$$

Nucleon exchange ( $I=\frac{1}{2}, J=\frac{1}{2}$ )

The matrix obtained with

$$\mathcal{H}_I = g_{\pi NN} \bar{\psi} \gamma_5 \tau \psi \cdot \phi \quad ,$$

nucleon propagator

$$\frac{i}{(2\pi)^4} \frac{1}{\not{p} - m}$$

and vertex functions

$$g_{\pi NN} \gamma_5 \tau_\alpha (2\pi)^4 \delta^4(p_2 - p - q_1) \quad ,$$

$$g_{\pi NN} \gamma_5 \tau_\beta (2\pi)^4 \delta^4(p_1 - p - q_2)$$

is given by

$$S_{fi} = -i(2\pi)^4 \delta^4(p_1 + q_1 - p_2 - q_2) \left\{ \frac{2m}{(2\pi)^6 \sqrt{2E(p_1)2E(p_2)2\omega_1 2\omega_2}} \right\} \\ \times \bar{u}_f(p_2) \left\{ \frac{q_1 + q_2}{2} \frac{g_{\pi NN}^2 \tau_\alpha \tau_\beta}{u - m^2} \right\} u_i(p_1) \quad ,$$

giving

$$\left. \begin{aligned} A \left( \frac{1}{2}; \frac{3}{2} \right) &= 0 \\ B \left( \frac{1}{2}; \frac{3}{2} \right) &= (1; -2) \frac{g_{\pi N \bar{N}}^2}{m^2 - u} \end{aligned} \right\} \quad (3.27)$$

The coupling constant is

$$\frac{g_{\pi N \bar{N}}^2}{4\pi} = 14.6 \quad , \quad (3.28)$$

and the mass of nucleon is

$$m = 6.7 \quad (939 \text{ MeV}) \quad . \quad (3.29)$$

$N^*$  resonance exchange ( $I=\frac{3}{2}$ ,  $J=\frac{3}{2}$ )

If there is an  $N^*$  resonance (mass  $m_{33} = 8.8$ ) dominating the low energy region of the s-channel, it is sufficient to keep only the  $I=\frac{3}{2}$ ,  $J=\frac{3}{2}$ ,  $\ell=1$  term in the expansion of  $f_1$  and  $f_2$  in Equation (3.10), i.e.

$$\left. \begin{aligned} \text{Im } f_1(s) &= 3x \text{Im } f_{J=1+}^{I=\frac{3}{2}}(s), \\ \text{Im } f_2(s) &= -\text{Im } f_{1+}^{\frac{3}{2}}(s) \end{aligned} \right\} \quad (3.30)$$

Substitution into Equation (3.6) gives

$$\begin{pmatrix} \text{Im } A(s,t,u) \\ \text{Im } B(s,t,u) \end{pmatrix} = \begin{pmatrix} \text{Im } A_{\frac{3}{2}}^{\frac{3}{2}}(s,t,u) \\ \text{Im } B_{\frac{3}{2}}^{\frac{3}{2}}(s,t,u) \end{pmatrix} = 4\pi \text{Im } f_{1+}^{\frac{3}{2}} \begin{pmatrix} \frac{W+m}{E+m} 3x + \frac{W-m}{E-m} \\ \frac{1}{E+m} 3x - \frac{1}{E-m} \end{pmatrix} \quad (3.31)$$

The expression for  $\text{Im } f_{1+}^{\frac{3}{2}}(s)$  obtained with a narrow width approximation is given by<sup>7)</sup>

$$\text{Im } f_{1+}^{\frac{3}{2}}(s) = \frac{8\pi m_{33}}{3} \left( \frac{g_{\pi NN}^2}{4} \right) \frac{1}{4m^2} (E_{33}^2 - m^2) \delta(s - m_{33}^2). \quad (3.32)$$

where  $E_{33}$  is the kinetic energy of the nucleon in  $N^*$  resonance.

For an  $N^*$  dominating the  $u$ -channel, the expressions for  $\text{Im } A(u,t,s)$ ,  $\text{Im } B(u,t,s)$  are the same as Equation (3.31) with exchange  $s \longleftrightarrow u$ , since the  $u$ -channel is obtained from the  $s$ -channel by exchange  $q_1 \longleftrightarrow q_2$ . The contribution of this resonance in the  $u$ -channel to the  $s$ -channel is obtained with crossing matrix (A.18). This gives

$$\begin{aligned} \begin{pmatrix} A_{\frac{1}{2}}^{\frac{1}{2}}(s,t,u) \\ A_{\frac{3}{2}}^{\frac{3}{2}}(s,t,u) \end{pmatrix} &= \begin{pmatrix} \frac{4}{3} \\ \frac{1}{3} \end{pmatrix} \frac{1}{\pi} \int_{(m+1)^2}^{\infty} \frac{\text{Im } A_{\frac{3}{2}}^{\frac{3}{2}}(u',t,s)}{u' - u} du' \\ &= \begin{pmatrix} \frac{4}{3} \\ \frac{1}{3} \end{pmatrix} \frac{8\pi\gamma_{33}}{m_{33}^2 - u} \left\{ (m_{33} - m)(E_{33} + m)^2 + \frac{3}{2}(m_{33} + m) \left[ m^2 + 1 - \frac{m_{33}^2}{2} - s \right. \right. \\ &\quad \left. \left. + \frac{(m^2 - 1)^2}{2m_{33}^2} \right] \right\} \quad (3.33) \end{aligned}$$

$$\begin{pmatrix} B^{\frac{1}{2}}(s,t,u) \\ B^{\frac{3}{2}}(s,t,u) \end{pmatrix} = \begin{pmatrix} -\frac{4}{3} \\ -\frac{1}{3} \end{pmatrix} \frac{8\pi\gamma_{33}}{m_{33}^2 - u} \left\{ -(E_{33} + m)^2 + \frac{3}{2} \left[ m^2 + 1 - \frac{m_{33}^2}{2} - s + \frac{(m^2 - 1)^2}{2m_{33}^2} \right] \right\} \quad (3.34)$$

where

$$\gamma_{33} = \frac{4m_{33}}{3(E_{33} + m)} \left( \frac{g_{\pi N \bar{N}}^2}{4\pi} \right) \frac{1}{4m^2} \approx 0.07 .$$

For the sake of comparison with results in Ref. 9-11, a smaller value  $\gamma_{33} = 0.06$  will be used. This is partially justified since Coulter and Shaw<sup>12)</sup> have shown that the detailed shape of the  $N^*$  resonance reduces its contribution to the direct channel by 25%.

The summation of contributions to  $A(s,t,u)$ ,  $B(s,t,u)$  from  $\sigma$ ,  $\rho$ ,  $N$  and  $N^*$  in the crossed channels is

$$\begin{aligned} A \left( \frac{1}{2}; \frac{3}{2} \right) &= (1;1) \frac{2g_{\sigma N \bar{N}} g_{\sigma \pi \pi}}{m_{\sigma}^2 - t} + (2;-1) \frac{6\pi\gamma_2}{m_{\rho}^2 - t} [2s + t - 2m^2 - 2] \\ &+ \left( \frac{4}{3}; \frac{1}{3} \right) \frac{8\pi\gamma_{33}}{m_{33}^2 - u} \{ (m_{33} - m) (E_{33} + m)^2 \\ &+ \frac{3}{2} (m_{33} + m) \left[ m^2 + 1 - \frac{m_{33}^2}{2} - s + \frac{(m^2 - 1)^2}{2m_{33}^2} \right] \} , \quad (3.35) \end{aligned}$$

$$\begin{aligned} B \left( \frac{1}{2}; \frac{3}{2} \right) &= (1;-2) \frac{g_{\pi N \bar{N}}^2}{m^2 - u} + (2;-1) (-12\pi) \frac{\gamma_1 + 2m\gamma_2}{m_{\rho}^2 - t} + \left( -\frac{4}{3}; -\frac{1}{3} \right) \\ &\times \frac{8\pi\gamma_{33}}{m_{33}^2 - u} \left\{ -(E_{33} + m)^2 + \frac{3}{2} \left[ m^2 + 1 - \frac{m_{33}^2}{2} - s + \frac{(m^2 - 1)^2}{2m_{33}^2} \right] \right\} , \quad (3.36) \end{aligned}$$

$$\left. \begin{aligned}
 \gamma_1 &= -0.84 \quad , & \gamma_2 &= 0.27 \gamma_1 \quad , & \gamma_{33} &= 0.06 \quad , \\
 m_\sigma &= 4.0 \quad , & m_\rho &= 5.4 \quad , & m &= 6.7 \quad , \\
 m_{33} &= 8.8 \quad , & \frac{g_{\pi N \bar{N}}^2}{4\pi} &= 14.6 \quad , \\
 G_\sigma &= \frac{g_{\sigma \pi \pi} g_{\sigma N \bar{N}}}{4\pi} = \pm 12 \quad .
 \end{aligned} \right\} (3.37)$$

These contributions are regular in the physical region, since none of the denominators vanishes for  $s \geq (m+1)^2$ .

#### D. N/D Dispersion Relations

We would like to work in the  $W$ -plane and derive the N/D partial wave dispersion relations for  $f_{\ell\pm}$ . The reason for working in the  $W$ -plane is to avoid kinematical singularities which would arise in computing quantities such as  $\sqrt{W^2}$ , since the expansion of  $f_{\ell\pm}$  in terms of  $A_\ell$ ,  $B_\ell$  involves factors  $E_{\ell m}$  coming from Dirac spinors. These singularities are nowhere given or bounded by unitarity, so that a self-consistent calculation in the  $W^2$ -plane would be very much complicated. Working on partial wave amplitudes  $f_{\ell\pm}$  also makes it simple to impose unitarity condition which reads, from Equation (3.12),

$$\text{Im} (f_{\ell\pm}^{-1}) = - \frac{2k}{1+\eta_{\ell\pm}} \quad . \quad (3.38)$$

For a given total angular momentum state  $J$ , we would solve for  $f_{\ell+}(W)$  in the positive energy region, and

extract the  $f_{(\ell+1)-}(W)$  results from the negative energy region with the aid of Equation (3.19).

To ensure that the computed partial waves has the correct threshold behaviour, it is found convenient to work with a new amplitude  $h_{\ell+}(W)$  obtained from  $f_{\ell+}$  by multiplication with a threshold factor, i.e.,

$$h_{\ell+}(W) = \frac{k}{\rho_{\ell+}(W)} f_{\ell+}(W) \quad (3.39)$$

where

$$\rho_{\ell+}(W) = \frac{(E+m)k^{2J}}{W^{2J}} \quad (3.40)$$

This new amplitude satisfies the relations

$$h_{\ell+}(z^*) = h_{\ell+}^*(z) \quad (3.41)$$

and

$$h_{\ell+}(-W + i\epsilon) = \frac{-W^{2J}}{(E-m)k^{2J-1}} f_{(\ell+1)-}^*(W + i\epsilon) \quad (3.42)$$

so that a solution of  $h_{\ell+}$  which is constant at  $W = (m\pm 1)$  and  $W = -(m\pm 1)$  would give

$$\left. \begin{aligned} \delta_{\ell+}(W) &\sim k^{2J} = k^{2\ell+1} \quad , \\ \delta_{(\ell+1)-}(W) &\sim (E-m)k^{2J} \sim k^{2(\ell+1)+1} \quad , \end{aligned} \right\} \quad (3.43)$$

at the thresholds of the two  $\ell = J \pm \frac{1}{2}$  orbital angular



momentum states. Writing

$$h_{\ell+}(z) = \frac{N_{\ell+}(z)}{D_{\ell+}(z)} \quad (3.44)$$

with  $N_{\ell+}$  containing the unphysical U and inelastic I cuts, and  $D_{\ell+}$  containing the unitarity P-cuts and at the same time satisfying the relation

$$\frac{D_{\ell+}^*(W)}{D_{\ell+}(W)} = e^{2i\delta_{\ell+}(W)}, \quad (3.45)$$

one gets

$$\left. \begin{aligned} \text{Im } D_{\ell+}(W) &= -\frac{2\rho_{\ell+}(W)}{1+\eta_{\ell+}(W)} \text{Re } N_{\ell+}(W), \quad |W| > (m+1), \\ \text{Im } N_{\ell+}(W) &= \frac{1-\eta_{\ell+}(W)}{2\rho_{\ell+}(W)} \text{Re } D_{\ell+}(W), \quad |W| > W_I, \end{aligned} \right\} (3.46)$$

and otherwise

$$\text{Im } N_{\ell+}(z) = D_{\ell+}(z) \text{Im } h_{\ell+}(z). \quad (3.47)$$

The dispersion relations for  $N_{\ell+}(z)$ ,  $D_{\ell+}(z)$  with normalization

$$D_{\ell+}(z=0) = 1 \quad (3.48)$$

and

$$\begin{aligned} D_{\ell+}(z) &= 1 + \frac{z}{\pi} \left\{ \int_{-\infty}^{-(m+1)} + \int_{(m+1)}^{\infty} \right\} \frac{dW'}{W'(W'-z)} \\ &\times \left[ -\frac{2\rho_{\ell+}(W')}{1+\eta_{\ell+}(W')} \text{Re } N_{\ell+}(W') \right] \end{aligned} \quad (3.49)$$

$$N_{\ell+}(z) = \frac{1}{\pi} \int_{\mathcal{U}} \frac{dz'}{z'-z} [D_{\ell+}(z) \cdot \text{Im } h_{\ell+}(z)] \\ + \frac{1}{\pi} \int_{\mathcal{I}} \frac{dW'}{W'-z} \left[ \frac{1-\eta_{\ell+}(W')}{2\rho_{\ell+}(W')} \text{Re } D_{\ell+}(W') \right]. \quad (3.50)$$

On substituting the expression for  $D_{\ell+}$  into  $N_{\ell+}$  and rearranging the orders of integration, one gets

$$\frac{2\eta_{\ell+}(W)}{1+\eta_{\ell+}(W)} \text{Re } N_{\ell+}(W) = B_{\ell+}(W) + \frac{1}{\pi} \left\{ \int_{-\infty}^{-(m+1)} + \int_{(m+1)}^{\infty} \right\} \frac{dW'}{W'-W} \times \\ [B_{\ell+}(W') - \frac{W}{W'} B_{\ell+}(W)] \frac{2\rho_{\ell+}(W') \text{Re } N_{\ell+}(W')}{1+\eta_{\ell+}(W')} \quad (3.51)$$

with

$$B_{\ell+}(W) = \text{Re } h_{\ell+}^U(W) + \frac{P}{\pi} \left\{ \int_{-\infty}^{-WI} + \int_{WI}^{\infty} \right\} \frac{dW'}{W'-W} \left[ \frac{1-\eta_{\ell+}(W')}{2\rho_{\ell+}(W')} \right] \quad (3.52)$$

where  $WI$  is the inelastic threshold. The quantity  $\text{Re } h_{\ell+}^U(W)$  is the contribution to  $\text{Re } h_{\ell+}(W)$  from the unphysical cuts. In the present calculation,

$$\text{Re } h_{\ell+}^U(W) = \frac{W^{2J-1}}{(E+m)k^{2J-1}} \frac{1}{16\pi} \{ (E+m)[A_{\ell}^U + (W-m)B_{\ell}^U] \\ + (E-m)[-A_{\ell+1}^U + (W+m)B_{\ell+1}^U] \}, \quad (3.53)$$

$$[A_{\ell}^U, B_{\ell}^U] = \int_{-1}^1 [A, B] P_{\ell}(x) dx \quad (3.13')$$

with  $A, B$  given by Equations (3.35) and (3.36).

To solve for  $N_{\ell+}(W)$  and  $D_{\ell+}(W)$ , one first computes  $B_{\ell+}(W)$  from Equations (3.35), (3.36), (3.13'), (3.53) and (3.52) in this order. The solution for  $\text{Re } N_{\ell}(W)$  can then be obtained from Equation (3.51). Values for  $\text{Re } D_{\ell+}(W)$ ,  $\text{Im } N_{\ell+}(W)$  and  $\text{Im } D_{\ell+}(W)$  then follow easily.

#### E. Calculation and Results

With A, B given by Equations (3.35) and (3.36) respectively, the integral in Equation (3.51) is divergent and a cut-off WC is introduced to yield results depending on its value. This same cut-off applied to the integral in Equation (3.52) imposes, at  $\pm WC$ , a condition  $\eta \rightarrow 1$  which can be relaxed by taking the limits of the integral to  $\pm\infty$  instead. For numerical purposes the integral in this equation is cut-off at 1500 (notation WIC will be used for this cut-off). The values of  $\text{Re } N_{\ell+}$  ( $|W| < 14$ ) calculated with this value of cut-off is found to differ from those calculated with  $WIC = 2500$  by less than 0.5%. Once WC and WIC are fixed,  $\text{Re } N_{\ell+}$  is solved by matrix inversion with 50 to 90 meshes. Values of  $\eta$  up to  $W \approx 15$  are taken from Ref. (5), and higher energy values are represented by  $\eta = \text{constant}$ . The results can be divided into four separate cases:

- (1) Elastic unitarity with exchange of  $\rho$ , N and  $N^*$

Here one finds two different values of cut-off.  $WC = 18.5$  and  $25.1$ , which produce  $N^*$  at  $W = 8.8$  (1236 MeV

centre of mass energy) in  $P_{33}$  channel (Figure 12). The lower cut-off gives the same results as in Ref. (9) to (11), and produces the nucleon as a bound state in  $P_{11}$  channel. The higher cut-off, however, gives positive scattering lengths  $a_1$  and  $a_3$  in  $S_{11}$  and  $S_{31}$  channels respectively, and at the same time the bound state nucleon pole moves above threshold to give a  $P_{11}$  resonance (Figures 12 and 14 to 21).

(2) Inelastic unitarity with exchange of  $\rho$ ,  $N$  and  $N^*$

With inelasticity included, the  $P_{33}$  and  $D_{33}$  waves were computed first by assigning values to  $\eta$  ( $W > 15.5$ ) for these channels in such a manner that the minimum of the curve for output  $P_{33}$  resonance position plotted as a function of  $WC$  appears at  $W = 8.8$  (Figure 13). The value of cut-off at this minimum is then used to compute the other  $J \leq \frac{3}{2}$  partial waves. The results for  $P_{13}$ ,  $P_{31}$ ,  $P_{33}$  and  $D_{33}$  partial waves up to 1500 MeV pion laboratory energy are found to be in better agreement with experiments than in Reference (10). In the case of  $S_{31}$  wave, inelasticity tends to make the results worse unless a lower cut-off  $WC = 18$  is used, in which case a very good fit to experimental results for both  $S_{31}$  and  $P_{31}$  waves can be obtained. It may be noted from Table I that the computed values of  $WC$  in the

$J=\frac{3}{2}$ ,  $I=\frac{3}{2}$  waves are around 21.0, and that a choice  $\eta=1$  for  $W > 15.5$  in  $S_{31}$  has been made in using a cut-off  $WC = 21.1$ . In the coupled  $S_{11}$  and  $P_{11}$  waves, adjusting  $\eta$  ( $W > 14.5$ ) in these channels to obtain a bound nucleon at  $W = 6.7$  in  $P_{11}$  gives negative values of phase shifts for all energies in both channels, in disagreement with experimental results. If  $\eta$  ( $W > 14.5$ ) in these channels are adjusted to give a correct value of scattering length  $a_1 = 0.18$  in  $S_{11}$ , the nucleon pole is pushed above the threshold to give a  $P_{11}$  resonance. It is not possible to produce a  $D_{13}$  resonance in this calculation.

(3) Elastic unitarity with exchange of  $\sigma$ ,  $\rho$ ,  $N$  and  $N^*$

The main reason for including the isoscalar  $\sigma$ -meson in the potential is to study its effect on the coupled  $S_{11}$ ,  $P_{11}$  waves. Two values of the coupling constant  $G_\sigma$ ,  $G_\sigma = \pm 12$ , are considered and the cut-off  $WC$  is again computed from the coupled  $P_{33}$ ,  $D_{33}$  waves by demanding a  $P_{33}$  resonance at  $W = 8.8$ . The results show that the effect of the  $\sigma$ -meson with the same cut-off is to shift the computed  $N^*$  resonance position down if  $G_\sigma$  is positive (Figure 13). It may be noted that there is no value of cut-off which produces the  $N^*$  at  $W = 8.8$  if  $G_\sigma = -12$ . The cut-off's for  $G_\sigma = 12$  are  $WC = 16.3$

and 27.7, and the  $J \leq \frac{3}{2}$  phase shifts computed with these cut-offs are similar to those in case (1) with WC = 18.5 and 25.1 respectively. For a given cut-off WC, it is found that the effect of  $\sigma$ -meson is to make the nucleon more tightly bound in  $P_{11}$  if  $G_\sigma$  is positive. To be more specific, with WC = 21.1,  $G_\sigma = 12$  gives a bound state nucleon at  $W = 7.5$  while  $G_\sigma = 0$  gives a resonance at  $W = 8.1$  (the nucleon bound state is lost), and  $G_\sigma = -12$  results in the phase shift rising to a maximum of about  $85^\circ$  at  $W = 9.6$  (Figures 15 and 23).

(4) Inelastic unitarity with exchange of  $\sigma$ ,  $\rho$ , N and  $N^*$

With inelasticity and requiring that there be only one cut-off WC giving  $N^*$  at  $W = 8.8$ , the effect of increasing  $G_\sigma$  ( $G_\sigma > 0$ ) is to require the high energy  $D_{33}$  partial waves to be more and more inelastic, and correspondingly the high energy  $P_{33}$  wave less and less inelastic (see Table I). The computed cut-offs are around 20.5. It is also found that a positive value of  $G_\sigma$  makes the nucleon more tightly bound in  $P_{11}$  channel. For example, with WC = 21.1 and requiring  $a_1 = 0.18$  in  $S_{11}$ ,  $G_\sigma = 12$  gives a bound state nucleon at  $W = 7.6$ ,  $G_\sigma = 0$  gives a  $P_{11}$  resonance at  $W = 8.6$  while  $G_\sigma = -12$  has the phase shift rising to a maximum of about  $80^\circ$  at  $W = 10.1$ .

## TABLES

VALUES OF INELASTIC PARAMETERS FOR  $W > 15.0$  AND CUT-OFFS  
FOR DIFFERENT PARTIAL WAVES

Table I

$G_\sigma$	WC	2J	2I	$\eta_{\ell+}(W > 15.5)$	$\eta_{(\ell+1)-}(W > 15.5)$
12	20.1	3	3	1.00	0.54
-12	20.1	3	3	0.55	0.80
-12	20.9	3	3	0.63	1.00
0	21.1	3	3	0.94	1.00
0	21.1	3	3	0.89	0.80
0	21.1	3	3	0.82	0.90
0	21.1	3	1	0.10	0.80
0	21.1	1	3	0.60	1.00

Table II

$G_\sigma$	WC	2J	2I	$\eta_{0+}(W > 14.5)$	$\eta_{1-}(W > 14.5)$
12	21.1	1	1	0.62	0.69
0	21.1	1	1	0.32	0.75
-12	21.1	1	1	0.17	0.73

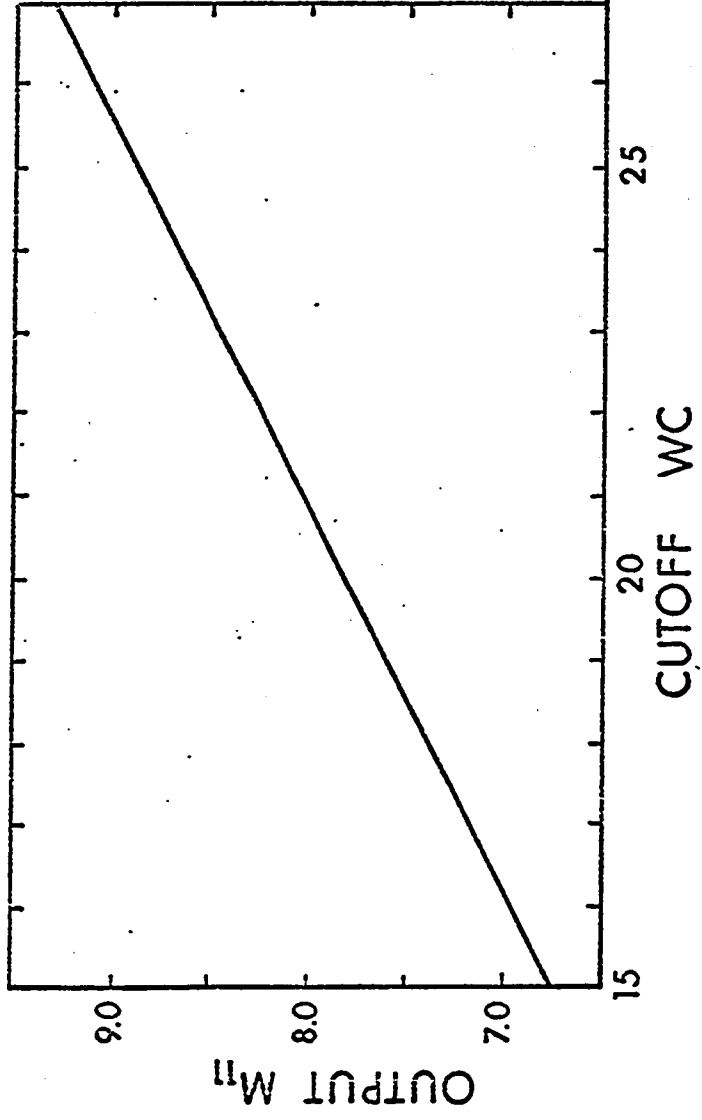


Figure 12



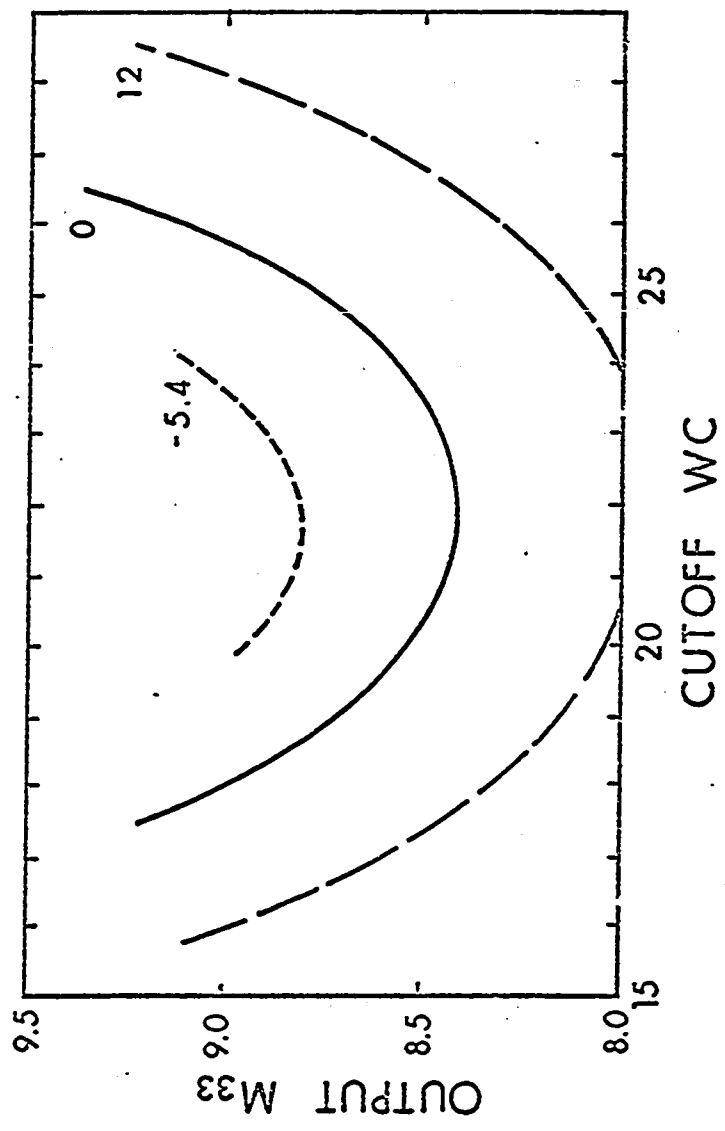


Figure 13

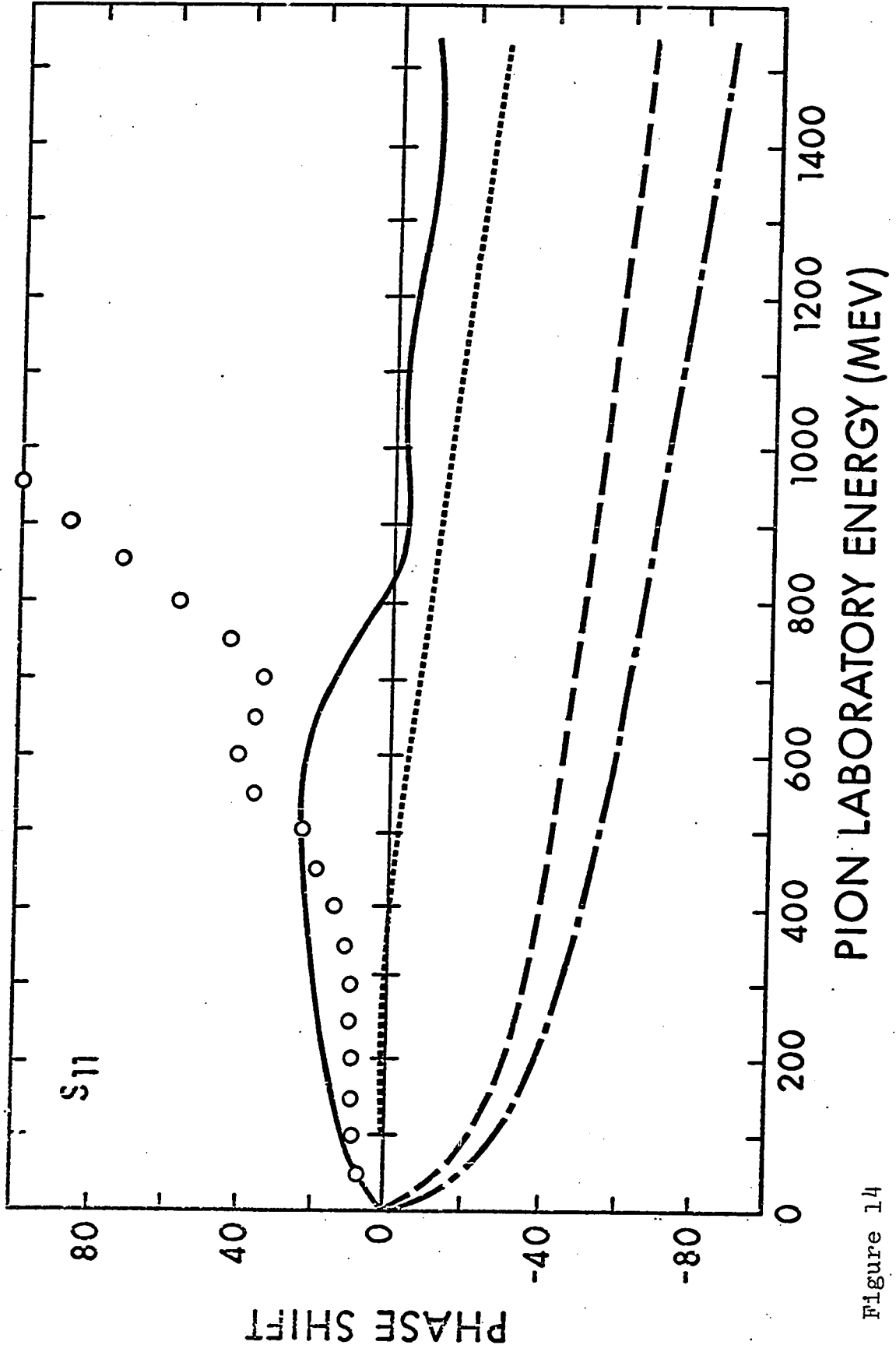


Figure 14

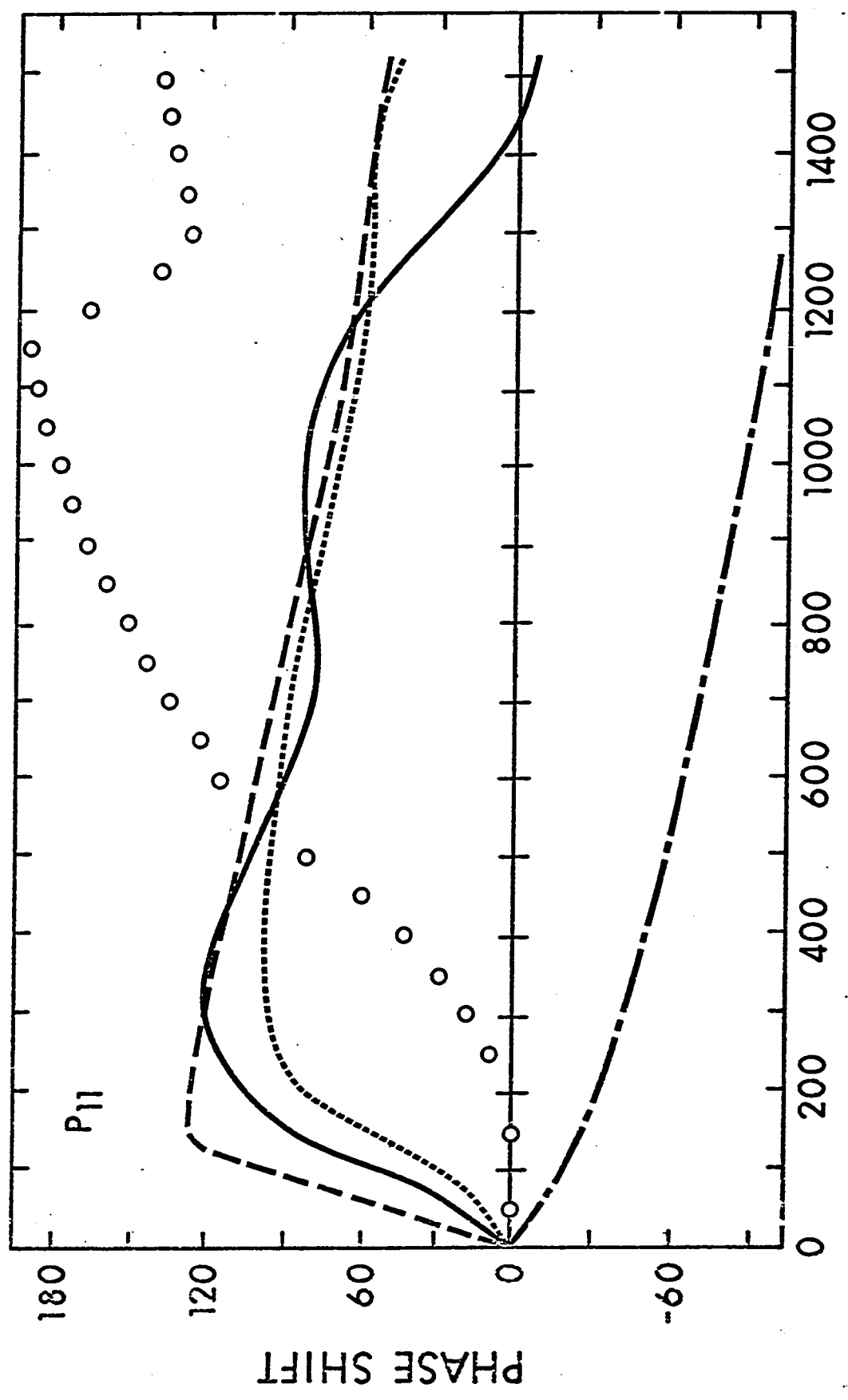


Figure 15

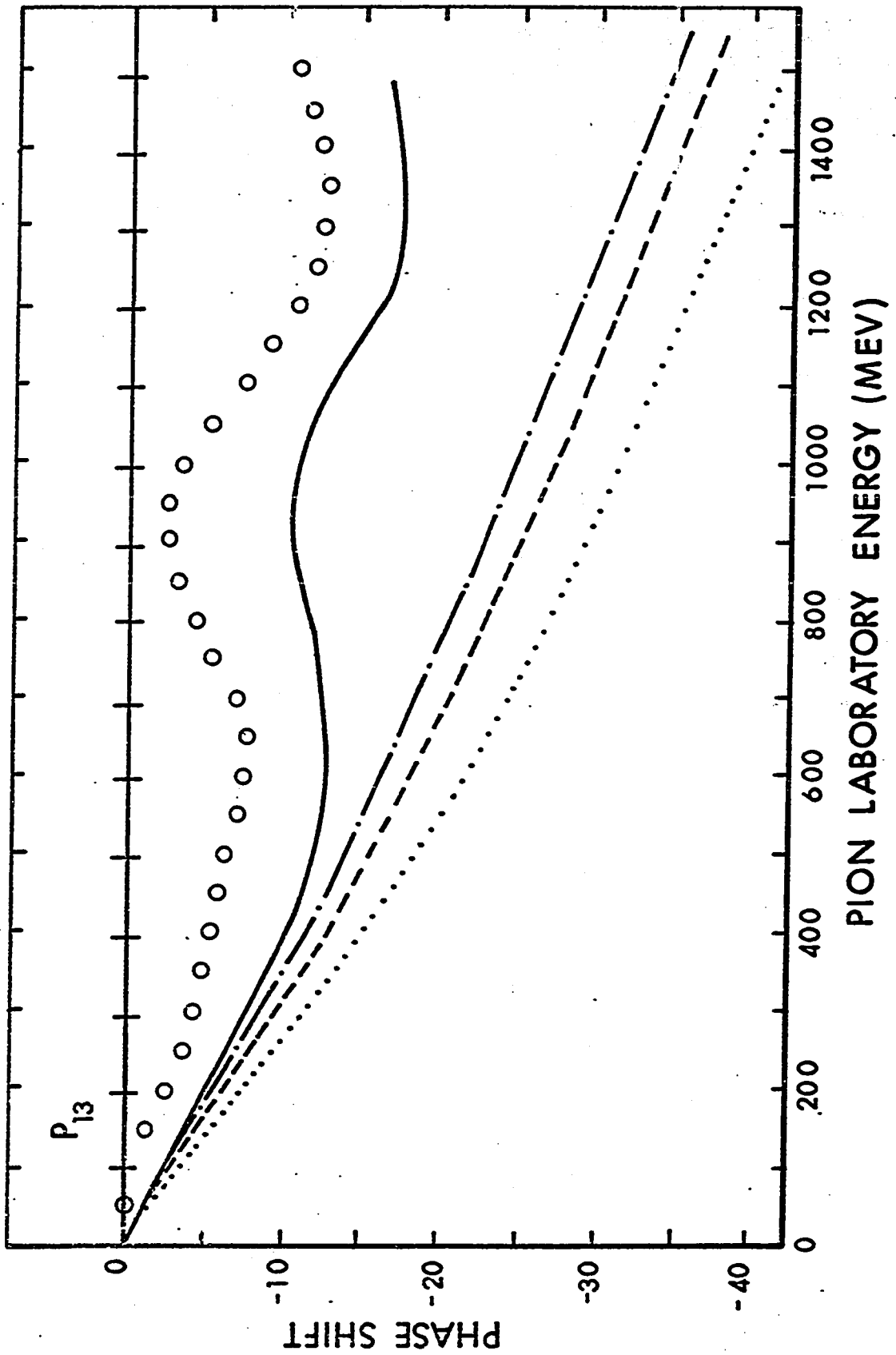


Figure 16

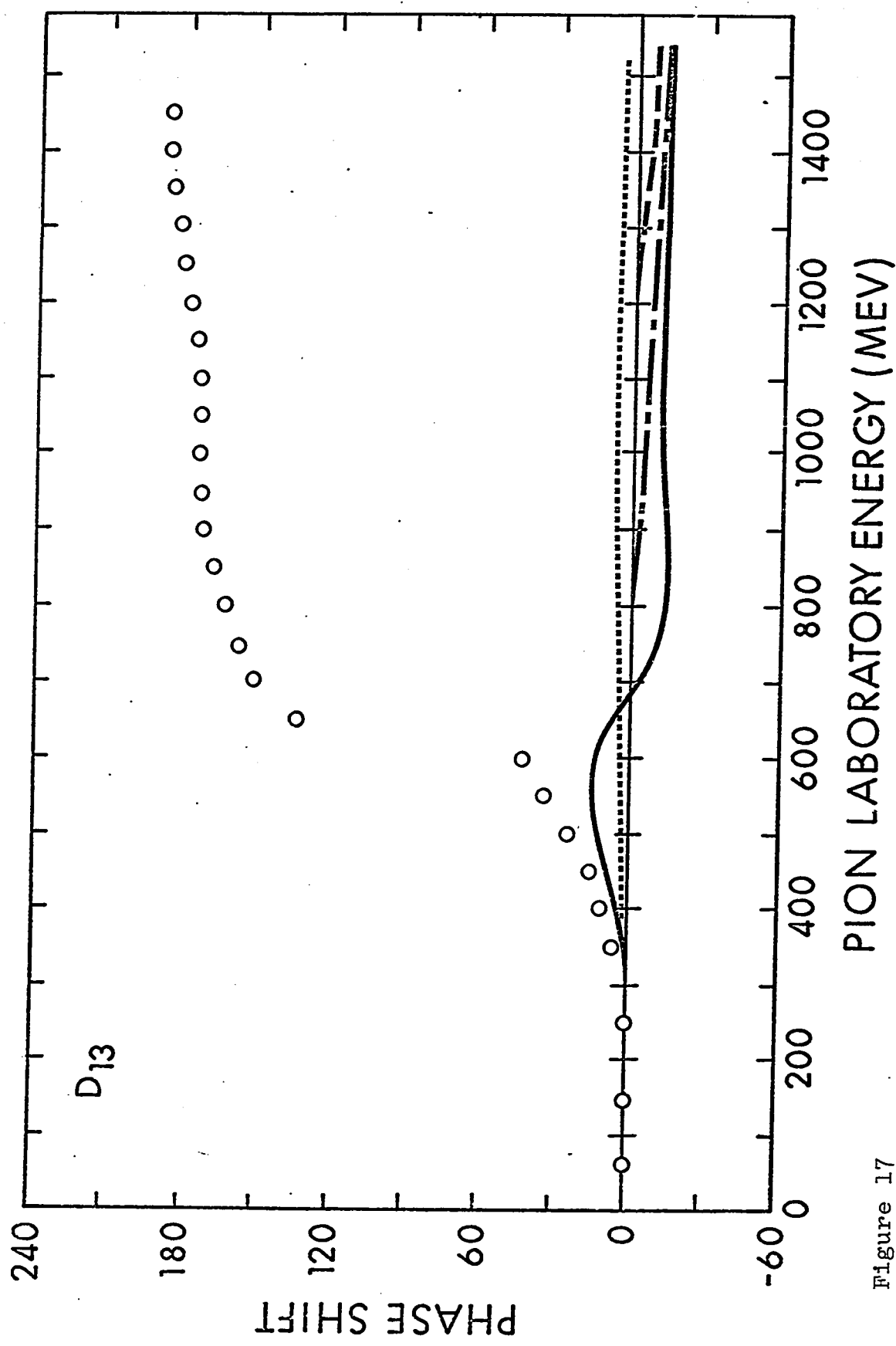


Figure 17

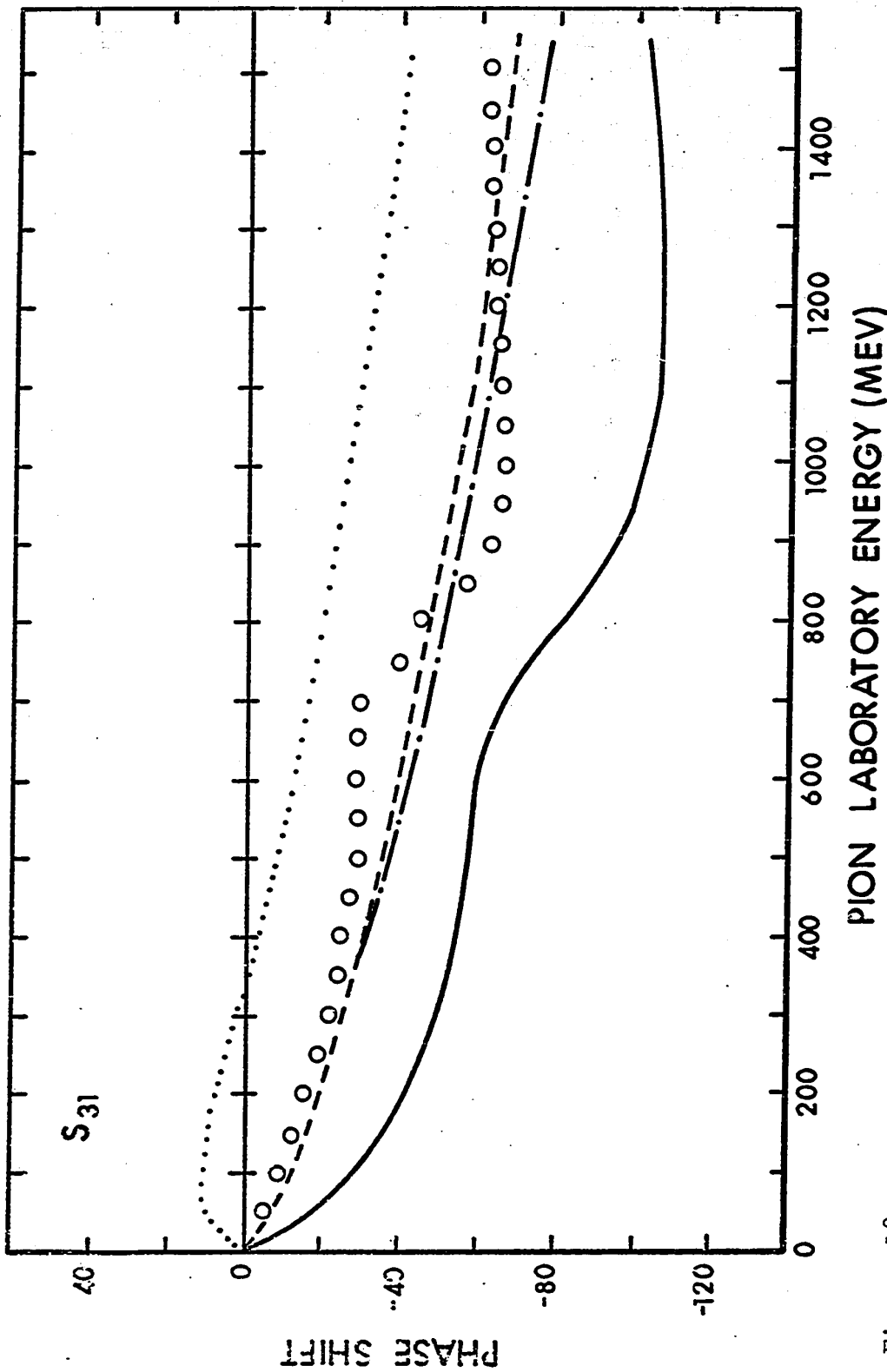


Figure 18

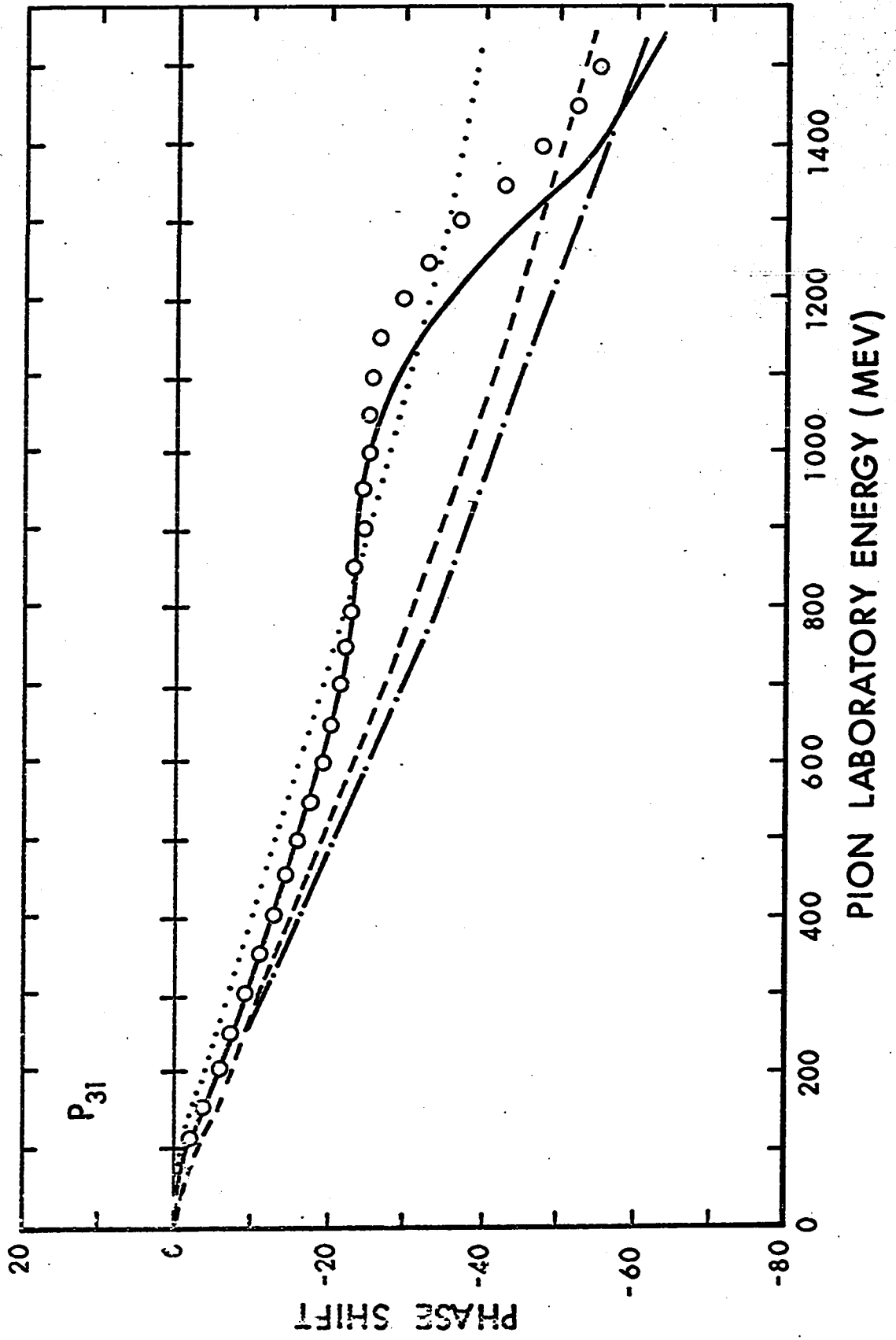


Figure 19

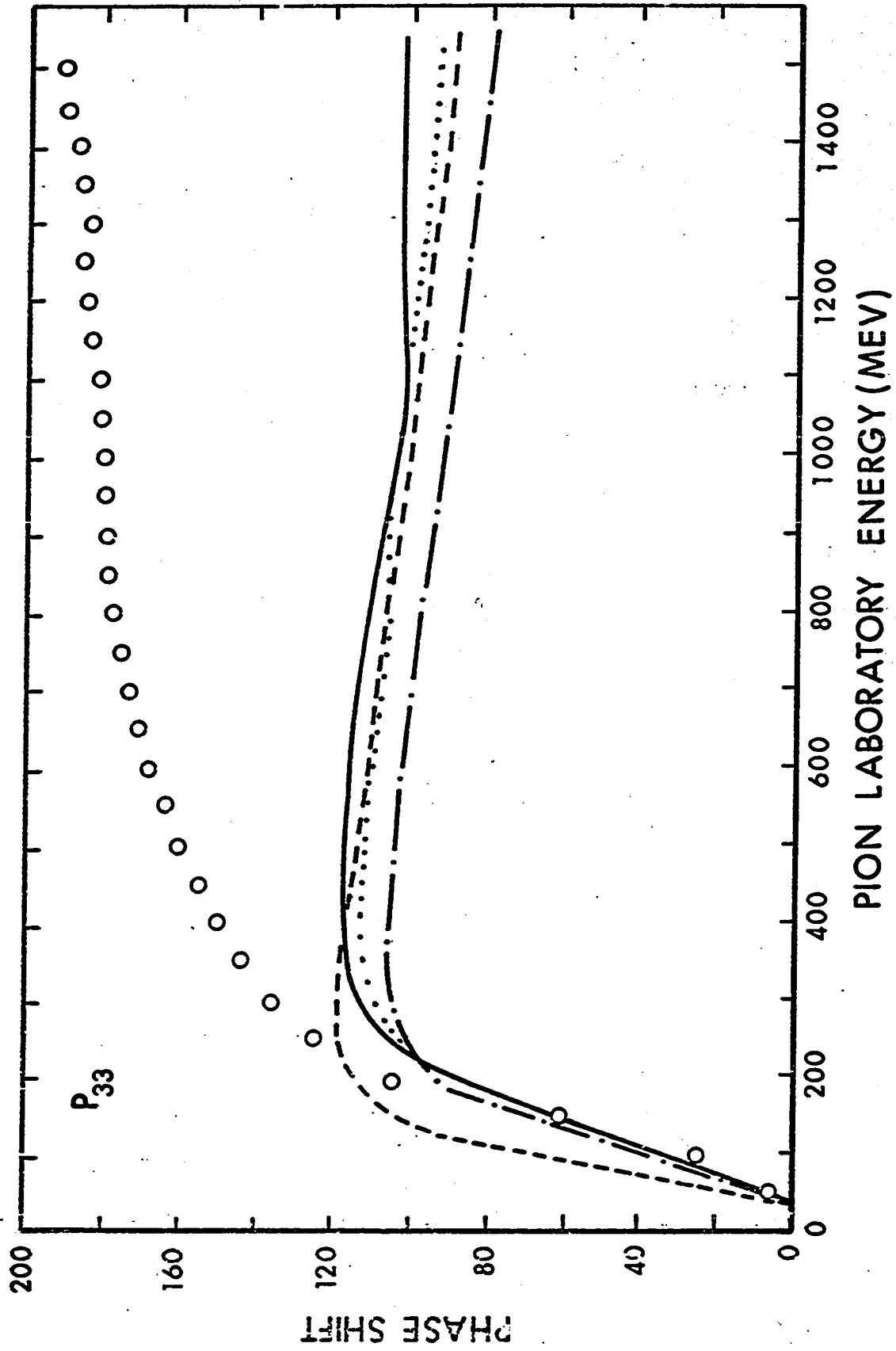


Figure 20



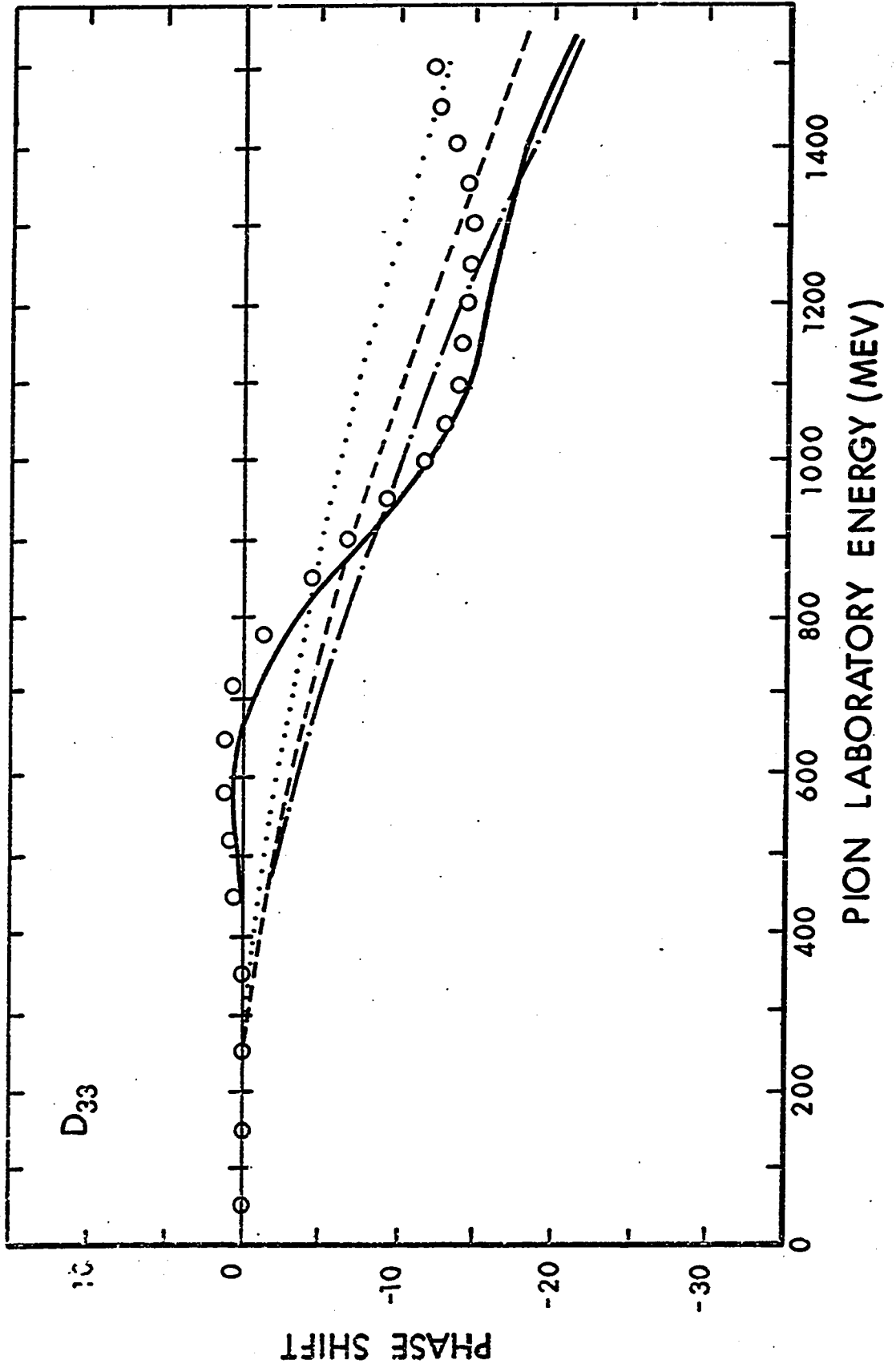


Figure 21

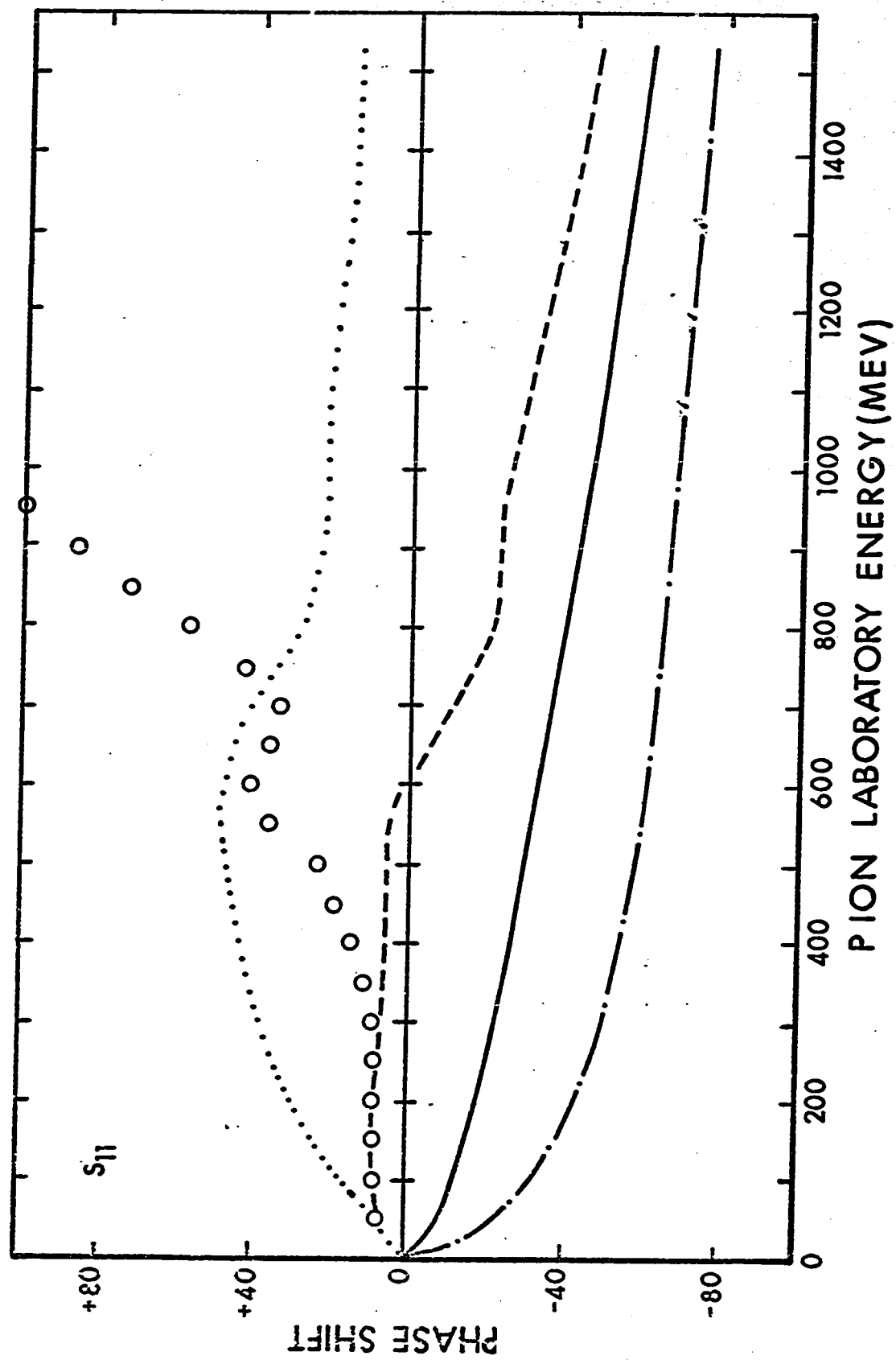


Figure 22

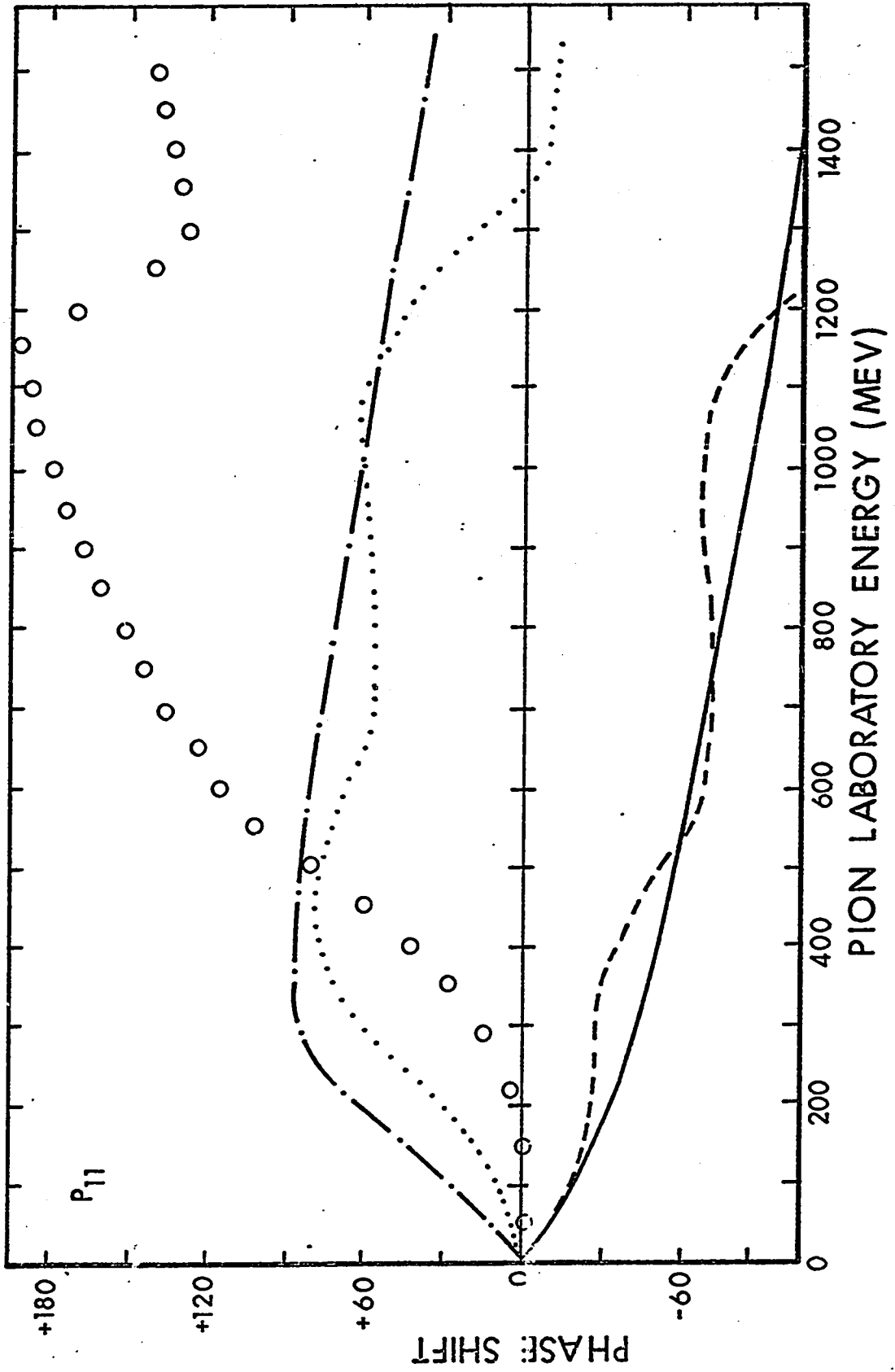


Figure 23

#### F. Conclusion

The foregoing analysis shows that one can obtain good results for the  $S_{31}$ ,  $P_{31}$ ,  $P_{13}$ ,  $P_{33}$  and  $D_{33}$  phase shifts with the inclusion of inelasticity above 700 MeV pion laboratory energy, and freedom to adjust the cut-offs for different coupled waves. The success of multi-channel calculations on  $P_{11}$  partial wave<sup>13-15)</sup>, and the non-equivalence of single- and multi-channel treatments<sup>23,24)</sup> confirms the general belief that one cannot secure both a dynamical bound nucleon and a  $P_{11}$  resonance in one-channel calculations.

## APPENDIX A

## MANDELSTAM REPRESENTATION OF INVARIANT AMPLITUDES

It was shown in Section 3B that the dynamics of  $\pi N$  scattering is contained in the invariant amplitudes  $A_{\beta\alpha}(s,t,u)$ ,  $B_{\beta\alpha}(s,t,u)$ . Ignoring isospin considerations, crossing symmetry implies that these amplitudes also describe physical scatterings  $\pi N \rightarrow \pi N$  in the  $u$ -channel region obtained by replacement  $q_1 \leftrightarrow -q_2$ , and  $\pi\pi \rightarrow N\bar{N}$  in the  $t$ -channel by replacement  $p_1 \leftrightarrow -q_2$ . To obtain a meaningful continuation of  $A$  and  $B$  from one physical region to the other, Mandelstam<sup>25)</sup> conjectured that  $A$ ,  $B$  are analytic functions of  $s$ ,  $t$  and  $u$ . All its singularities arise from bound states and kinematical cuts in the  $s$ ,  $t$ ,  $u$  channels. Hence,

$$\begin{aligned}
 B(s,t,u) = & \frac{R_s}{m^2-s} + \frac{R_u}{m^2-u} + \frac{1}{\pi^2} \int_{(m+1)^2}^{\infty} ds' \int_{(m+1)^2}^{\infty} du' \frac{B_{su}(s',u')}{(s'-s)(u'-u)} \\
 & + \frac{1}{\pi^2} \int_{(m+1)^2}^{\infty} ds' \int_4^{\infty} dt' \frac{B_{st}(s',t')}{(s'-s)(t'-t)} \\
 & + \frac{1}{\pi^2} \int_{(m+1)^2}^{\infty} du' \int_4^{\infty} dt' \frac{B_{ut}(u',t')}{(u'-u)(t'-t)} , \quad (A1)
 \end{aligned}$$

which can be rewritten in a one-dimensional fixed  $s$  dispersion relation

$$B(s,t,u) = \frac{R_s}{m^2-s} + \frac{R_u}{m^2-u} + \frac{1}{\pi} \int_4^\infty dt' \frac{B_t(s,t')}{t'-t} \\ + \frac{1}{\pi} \int_{(m+1)^2}^\infty du' \frac{B_u(s,u')}{u'-u}, \quad (A2)$$

with

$$B_t(s,t') = \frac{1}{\pi} \int_{(m+1)^2}^\infty ds' \frac{B_{st}(s',t')}{s'-s} \\ - \frac{1}{\pi} \int_{-\infty}^{(m-1)^2-t'} ds' \frac{B_{ut}(s',t')}{s'-s}, \quad (A3)$$

$$B_u(s,u') = \frac{1}{\pi} \int_{(m+1)^2}^\infty ds' \frac{B_{su}(s',u')}{s'-s} \\ - \frac{1}{\pi} \int_{-\infty}^{2m^2-2-u'} ds' \frac{B_{ut}(s',u')}{s'-s}. \quad (A4)$$

The expressions for  $A(s,t,u)$  are similar, with the exception that the poles in  $s$  and  $u$  are absent as a result of the pseudoscalar property of the pion. The double spectral functions  $B_{su}$ , etc., are real and vanish outside the regions whose asymptotic limits are the limits of the integrals in Equation (A1). A detailed discussion of these boundary curves is given in Reference (25).

When isospin is taken into account, the matrix

$$T_{\beta\alpha} = A_{\beta\alpha} + \frac{q_1 + q_2}{2} B_{\beta\alpha} \quad (\text{A5})$$

between final pion isospin index  $\beta$  and initial index  $\alpha$  can be decomposed into symmetric and antisymmetric parts

$$T_{\beta\alpha} = \delta_{\beta\alpha} T^+ + \frac{1}{2} [\tau_\beta, \tau_\alpha] T^- \quad (\text{A6})$$

Comparing with

$$T_{\beta\alpha} = T^{\frac{3}{2}} Q_{\beta\alpha}^{\frac{3}{2}} + T^{\frac{1}{2}} Q_{\beta\alpha}^{\frac{1}{2}} \quad (\text{A7})$$

and using Equations (B2), (B3)

$$\begin{pmatrix} T^+ \\ T^- \end{pmatrix} = \begin{pmatrix} \frac{1}{3} & \frac{2}{3} \\ \frac{1}{3} & -\frac{1}{3} \end{pmatrix} \begin{pmatrix} T^{\frac{1}{2}} \\ T^{\frac{3}{2}} \end{pmatrix}, \quad (\text{A8})$$

from which

$$\left. \begin{aligned} T_{\pi^+ p \rightarrow \pi^+ p} &= T^+ - T^- \\ T_{\pi^- p \rightarrow \pi^- p} &= T^+ + T^- \end{aligned} \right\} \quad (\text{A9})$$

Crossing relation between the s- and u-channel amplitudes can be obtained from the fact that the amplitude is invariant under exchange  $q_1 \leftrightarrow -q_2$ ,  $\beta \leftrightarrow \alpha$ . Since

$q_1 \leftrightarrow -q_2$  implies  $s \leftrightarrow u$ ,  $t \rightarrow t$ , the crossing relation reads,

$$T_{\beta\alpha}(s,t,u) = T_{\alpha\beta}(u,t,s) \quad (\text{A10})$$

which, with Equation (A5), gives

$$T^\pm(s,t,u) = \pm T^\pm(u,t,s) . \quad (\text{A11})$$

The amplitudes A and B are independent of each other, since B depends on nucleon spin but A does not. Their corresponding equations read

$$A_{\beta\alpha} = \delta_{\beta\alpha} A^+ + \frac{1}{2} [\tau_\beta, \tau_\alpha] A^- , \quad (\text{A12})$$

$$B_{\beta\alpha} = \delta_{\beta\alpha} B^+ + \frac{1}{2} [\tau_\beta, \tau_\alpha] B^- , \quad (\text{A13})$$

$$\begin{pmatrix} A^+ & B^+ \\ A^- & B^- \end{pmatrix} = \begin{pmatrix} \frac{1}{3} & \frac{2}{3} \\ \frac{1}{3} & -\frac{1}{3} \end{pmatrix} \begin{pmatrix} A^{1/2} & B^{1/2} \\ A^{3/2} & B^{3/2} \end{pmatrix}, \quad (\text{A14})$$

and

$$A^\pm(s,t,u) = \pm A^\pm(u,t,s) , \quad (\text{A15})$$

$$B^\pm(s,t,u) = \mp B^\pm(u,t,s) . \quad (\text{A16})$$

The inverse relations are

$$\begin{pmatrix} A^{1/2} & B^{1/2} \\ A^{3/2} & B^{3/2} \end{pmatrix} = \begin{pmatrix} 1 & 2 \\ 1 & -1 \end{pmatrix} \begin{pmatrix} A^+ & B^+ \\ A^- & B^- \end{pmatrix}, \quad (\text{A17})$$



$$\begin{pmatrix} A^{\frac{1}{2}}(s,t,u) & B^{\frac{1}{2}}(s,t,u) \\ A^{\frac{3}{2}}(s,t,u) & B^{\frac{3}{2}}(s,t,u) \end{pmatrix} = \begin{pmatrix} -\frac{1}{3} & \frac{4}{3} \\ \frac{2}{3} & \frac{1}{3} \end{pmatrix} \begin{pmatrix} A^{\frac{1}{2}}(u,t,s) & -B^{\frac{1}{2}}(u,t,s) \\ A^{\frac{3}{2}}(u,t,s) & -B^{\frac{3}{2}}(u,t,s) \end{pmatrix}$$

(A18)

## APPENDIX B

## PROJECTION OPERATORS

For  $\pi N$  scattering (Figure 9) with a bound state nucleon in the s-channel as an intermediate state, the matrix element  $S_{fi}$  contains a factor  $\tau_\beta \tau_\alpha$  which must be proportional to the projection operator  $Q_{\beta\alpha}^{\frac{1}{2}}$  onto isospin space  $I = \frac{1}{2}$  of the  $\pi N$  system. By property of projection operator

$$Q^{\frac{1}{2}} Q^{\frac{1}{2}} = Q^{\frac{1}{2}} \quad (B1)$$

one arrives at

$$Q^{\frac{1}{2}} = \frac{1}{3} \tau_\beta \tau_\alpha \quad (B2)$$

The projection operator  $Q^{3/2}$  onto isospin space  $I = 3/2$  is given by

$$Q^{3/2} = \delta_{\beta\alpha} - \frac{1}{3} \tau_\beta \tau_\alpha \quad (B3)$$

since it satisfies

$$Q^{3/2} Q^{3/2} = Q^{3/2} \quad (B4)$$

and

$$Q^{3/2} Q^{\frac{1}{2}} = Q^{\frac{1}{2}} Q^{3/2} = 0 \quad (B5)$$

With the aid of relations

$$\tau_\beta \tau_\alpha + \tau_\alpha \tau_\beta = 2 \delta_{\beta\alpha} \quad (B6)$$

$$\frac{1}{2} [\tau_\alpha, \tau_\beta] = i \epsilon_{\alpha\beta\gamma} \tau_\gamma \quad (B7)$$

one gets

$$\tau_{\alpha} \tau_{\beta} = 2 Q_{\beta\alpha}^{3/2} - Q_{\beta\alpha}^{1/2} \quad , \quad (\text{B8})$$

$$\delta_{\beta\alpha} = Q_{\beta\alpha}^{3/2} + Q_{\beta\alpha}^{1/2} \quad , \quad (\text{B9})$$

$$i \varepsilon_{\alpha\beta\gamma} \tau_{\gamma} = Q_{\beta\alpha}^{3/2} - 2 Q_{\beta\alpha}^{1/2} \quad . \quad (\text{B10})$$

## APPENDIX C

## AN ESTIMATE OF THE COUPLING

CONSTANTS  $g_{\sigma\pi\pi}$  AND  $G_{\sigma}$ 

The isoscalar  $\sigma$ -meson ( $I=0, J=0$ ) is a hypothetical particle with mass and decay width  $\Gamma(\sigma \rightarrow \pi\pi)$  in the range

$$\left. \begin{aligned} m_{\sigma} &= 500 - 900 \text{ MeV} , \\ \Gamma &= 100 - 450 \text{ MeV} . \end{aligned} \right\} \quad (C1)$$

The dipion resonance can be employed to take into account the strong attractive force between two pions. Its mass and coupling to the nucleons has been estimated by Bryan and Scott<sup>18)</sup> in the analysis of N-N scattering to be

$$m_{\sigma} = 560 \text{ MeV}$$

and

(C2)

$$\frac{g_{\sigma NN}}{4\pi} = 9.4 .$$

We would assume  $g_{\sigma NN}^2 = g_{\sigma NN}^2$  in our calculations.

In order to estimate the value of  $g_{\sigma\pi\pi}^2$  from the decay width  $\Gamma(\sigma \rightarrow \pi\pi)$ , consider the decay at rest of  $\sigma$ , momentum  $p$ , into two pions of momenta  $q_1, q_2$  with

$$\mathcal{H}_I = g_{\sigma\pi\pi} \sigma \phi \cdot \phi$$

$$p^{\mu} = (m_{\sigma}, \underline{0}) , \quad q_1^{\mu} = (\omega, \underline{q}) , \quad q_2^{\mu} = (\omega, -\underline{q})$$

and vertex function

$$2g_{\sigma\pi\pi}(2\pi)^4\delta^4(p - q_1 - q_2)$$

so that

$$S_{fi} = (-i) \left\{ \frac{1}{(2\pi)^{3/2}\sqrt{2\omega}} \right\} \left\{ \frac{1}{(2\pi)^{3/2}\sqrt{2\omega}} \right\} \times \\ \left\{ 2g_{\sigma\pi\pi}(2\pi)^4\delta^4(p - q_1 - q_2) \right\} \left\{ \frac{1}{(2\pi)^{3/2}\sqrt{2m_\sigma}} \right\} .$$

Recalling that the units are  $\hbar=c=\mu=1$  and the volume per particle is  $(2\pi)^3$ , the transition probability per unit time per unit volume is

$$\Gamma(\sigma \rightarrow \pi\pi) = \frac{1}{(2\pi)^{-3}V_T} \iint |S_{fi}|^2 d^3q_1 d^3q_2 = \frac{g_{\sigma\pi\pi}^2 \sqrt{m_\sigma^2 - 4}}{4\pi m_\sigma^2} . \quad (C3)$$

Hence

$$\frac{g_{\sigma\pi\pi}^2}{4\pi} = \frac{m_\sigma^2 \Gamma(\sigma \rightarrow \pi\pi)}{\sqrt{m_\sigma^2 - 4}} \approx 14.5 , \quad (C4)$$

$$G_\sigma = \frac{g_{\sigma\pi\pi} g_{\sigma NN}}{4\pi} \approx \pm 11.7 ,$$

with choice  $m_\sigma = 560 \text{ MeV} = 4\mu$ , and  $\Gamma = 420 \text{ MeV} = 3\mu$ .

It is not possible to determine the sign of  $G_\sigma$ , since only the quantities  $g_{\sigma NN}^2$  and  $g_{\sigma\pi\pi}^2$  can be calculated.

## REFERENCES

1. A. Donnachie, Pion-Nucleon Phase Shift Analysis  
Particle Interactions at High Energies, edited  
by T.W. Preist and L.L.J. Vick (Plenum Press,  
New York, 1967).
2. P. Bareyre, C. Bricman and G. Villet, Phys. Rev.  
165 (1968) 1730.
3. A. Donnachie, R.G. Kirsopp and C. Lovelace, Phys.  
Letters 26B (1968) 161.
4. Berkeley group (mentioned in Reference 5).
5. C. Lovelace, Nuclear Resonances and Low Energy  
Scattering. Proceedings of the Heidelberg  
International Conference on Elementary Particles  
(North-Holland Publishing Company, Amsterdam,  
1968)(session 3, page 79).
6. W.R. Frazer and J.R. Fulco, Phys. Rev. 119 (1960)  
1420.
7. S.C. Frautchi and J.D. Walecka, Phys. Rev. 120 (1960)  
1486.
8. E. Abers and C. Zemach, Phys. Rev. 131 (1963) 2305.
9. J.S. Ball and D.Y. Wong, Phys. Rev. 133 (1964) B179;  
138 (1965) AB4(E).
10. P.W. Coulter and G.L. Shaw, Phys. Rev. 141 (1966)  
1419.

11. S.R. Choudhury, A. Kumar and R.P. Saxema, Phys. Rev. 143 (1966) 1159.
12. P.W. Coulter and G.L. Shaw, Phys. Rev. 153 (1967) 1591.
13. J.S. Ball, Phys. Rev. 149 (1966) 1191.
14. J.S. Ball, G.L. Shaw and D.Y. Wong, Phys. Rev. 155 (1967) 1725.
15. J.S. Ball, R.C. Garg and G.L. Shaw, Phys. Rev. 177 (1969) 2258.
16. J. Rothleitner and B. Stech, Zeits. für Phys. 180 (1964) 375.
17. S.W. MacDowell, Phys. Rev. 116 (1960) 774.
18. R.A. Bryan and B.L. Scott, Phys. Rev. 135 (1964) B434.
19. B. Dutta-Roy and I.R. Lapidus, Phys. Rev. 169 (1968) 1357.
20. G.A. Smith and R.J. Manning, Phys. Rev. 171 (1968) 1399.
21. E. Malamud and P.E. Schlein, Phys. Rev. Letters 19 (1967) 1056.
22. J.S. Ball and D.Y. Wong, Phys. Rev. 130 (1963) 2112.
23. M. Bander, P.W. Coulter and G.L. Shaw, Phys. Rev. Letters 14 (1965) 270.
24. P. Hertel, Zeit. für Phys. 186 (1965) 288.
25. S. Mandelstam, Phys. Rev. 112 (1958) 1344; 115 (1959) 1741 and 1752.

CHAPTER TWO

EFFECTS OF INELASTICITY ON RESONANCES



## FIGURE CAPTIONS

Page

Figure 1 : Real part of S-wave phase shift vs  $s$ .

- Elastic unitarity,  $\lambda_1 = -500$ ,  $\lambda_2 = 3228.7$ ,  
 $s_1 = 150$ ,  $s_2 = 2000$ ;  
 $s_R = 25.0$ ,  $\Gamma = 10.59$ .  
 - - - (A)  $\alpha = 0.1$ ,  $a = 16$ ,  $b = 24$ ,  $\Delta = 4$ ;  $s_R = 20.6$ ,  $\Gamma = 1.09$   
 - - - (B)  $\alpha = 0.25$ ,  $a = 16$ ,  $b = 24$ ,  $\Delta = 4$ ;  $s_R = 19.6$ ,  $\Gamma = 0.18$   
 - - - (C)  $\alpha = 0.25$ ,  $a = 18$ ,  $b = 22$ ,  $\Delta = 2$ ;  $s_R = 20.2$ ,  $\Gamma = 0.26$

87

Figure 2 : Real part of S-wave phase shift vs  $s$ .

- Elastic unitarity;  $s_R = 25.0$ ,  $\Gamma = 10.59$   
 - - - (A)  $\alpha = 0.1$ ,  $a = 21$ ,  $b = 29$ ,  $\Delta = 4$ ;  $s_R = 24.6$ ,  $\Gamma = 0.92$   
 - - - (B)  $\alpha = 0.25$ ,  $a = 21$ ,  $b = 29$ ,  $\Delta = 4$ ;  $s_R = 24.0$ ,  $\Gamma = 0.26$   
 - - - (C)  $\alpha = 0.25$ ,  $a = 23$ ,  $b = 27$ ,  $\Delta = 2$ ;  $s_R = 24.6$ ,  $\Gamma = 0.22$

88

Figure 3 : Real part of S-wave phase shift vs  $s$ .

- Elastic unitarity;  $s_R = 25.0$ ,  $\Gamma = 10.59$   
 - - - (A)  $\alpha = 0.1$ ,  $a = 30$ ,  $b = 38$ ,  $\Delta = 4$ ;  $s_R = 33.0$ ,  $\Gamma = 1.21$   
 - - - (B)  $\alpha = 0.25$ ,  $a = 30$ ,  $b = 38$ ,  $\Delta = 4$ ;  $s_{R_1} = 21.7$ ,  $\Gamma_{R_1} = 16.0$ ,  
 $s_{R_2} = 32.9$ ,  $\Gamma_{R_2} = 0.24$   
 - - - (C)  $\alpha = 0.25$ ,  $a = 32$ ,  $b = 36$ ,  $\Delta = 2$ ;  $s_{R_1} = 23.3$ ,  $\Gamma_{R_1} = 12.8$ ,  
 $s_{R_2} = 33.2$ ,  $\Gamma_{R_2} = 0.43$

89

Figure 4 : Real part of P-wave phase shift vs s.

—————	Elastic unitarity, $\lambda_1=2.515$ , $s_1=100$ ; $s_R=25.0$ , $\Gamma=13.07$	
-----	$\alpha=0.1$ , $a=16$ , $b=24$ , $\Delta=4$ ; $s_{R_1}=26.0$ , $\Gamma=9.61$	
-----	$\alpha=0.25$ , $a=16$ , $b=24$ , $\Delta=4$ ; $s_{R_1}=16.0$ , $\Gamma_{R_1}=1.42$ , $s_{R_2}=27.3$ , $\Gamma_{R_2}=7.53$	
-----	$\alpha=0.25$ , $a=18$ , $b=22$ , $\Delta=2$ ; $s_{R_1}=17.6$ , $\Gamma_{R_1}=1.24$ , $s_{R_2}=26.3$ , $\Gamma_{R_2}=9.03$	91

Figure 5 : Real part of P-wave phase shift vs s.

—————	Elastic unitarity; $s_R=25$ , $\Gamma=13.07$	
-----	$\alpha=0.1$ , $a=21$ , $b=29$ , $\Delta=4$ ; $s_{R_1}=20.6$ , $\Gamma_{R_1}=3.41$ , $s_{R_2}=29.6$ , $\Gamma_{R_2}=9.41$	
-----	$\alpha=0.25$ , $a=21$ , $b=29$ , $\Delta=4$ ; $s_{R_1}=18.1$ , $\Gamma_{R_1}=30.3$ , $s_{R_2}=32.5$ , $\Gamma_{R_2}=9.47$	
-----	$\alpha=0.25$ , $a=23$ , $b=27$ , $\Delta=2$ ; $s_{R_1}=20.0$ , $\Gamma_{R_1}=3.82$ , $s_{R_2}=30.2$ , $\Gamma_{R_2}=8.85$	92

Figure 6 : Real part of P-wave phase shift vs s.

—————	Elastic unitarity; $s_R=25$ , $\Gamma=13.07$	
-----	$\alpha=0.1$ , $a=30$ , $b=38$ , $\Delta=4$ ; $s_{R_1}=22.5$ , $\Gamma_{R_1}=8.17$ , $s_{R_2}=39.6$ , $\Gamma_{R_2}=29.00$	
-----	$\alpha=0.25$ , $a=30$ , $b=38$ , $\Delta=4$ ; $s_R=20.4$ , $\Gamma=5.17$	
-----	$\alpha=0.25$ , $a=32$ , $b=36$ , $\Delta=2$ ; $s_R=21.8$ , $\Gamma=7.03$	93

Figure 7 : Output  $\delta$  evaluated with inelastic potential only.

## 1. INTRODUCTION

In the field of strong interaction physics resonances that can be understood in the elastic approximation are very few. The only such example in  $\pi N$  scattering is the  $N^*(1236 \text{ MeV})$  resonance which has been studied by various authors<sup>1)</sup>. When dynamical calculations were performed on other resonances such as the  $\rho$ -meson<sup>2)</sup> using elastic unitarity, the width invariably came out too large compared with experimental results. Since inelastic channels had been ignored, it was hoped that the results could be improved with the inclusion of inelasticity.

The effect of inelasticity on a resonance has not been investigated in the general case. While the correct approach is to solve a full multi-channel problem, the complexity of this calculation is enormous and forbidding. Special cases with two or three channels have been studied by many authors, notably Fulco, Shaw and Wong<sup>3)</sup>, and Nath and Der Sarkissian<sup>4)</sup>. In the examples examined Fulco et al. found that inelasticity moved resonances closer to the threshold with reduced widths; Nath and Der Sarkissian also found that the effect of inelasticity on a resonance was attractive, but the width could be increased or decreased. An example of single channel N/D calculation

with inelastic unitarity is the  $\rho$ -meson problem studied by Coulter and Shaw<sup>5)</sup>. It was found that the resonance width was reduced on inclusion of inelasticity.

The present work is a study of the effect of inelasticity on the position and the width of resonances in a more general scheme using a simple model. The model is so designed as to be (1) amenable to an analytic solution in the absence of inelasticity, and (2) to obviate the need for a cut-off. It is assumed that a single-channel calculation faithfully simulates the results of a multi-channel calculation. This precludes the possibility of the inelastic channel being so strong as to produce a bound state in the continuum region of the elastic channel.<sup>6)</sup>

## 2. KINEMATICS

Consider the s-channel elastic scattering of two equal mass, spinless particles with mass  $m$  and 4-momenta  $p_i$ ,

$$a_1 + a_2 \rightarrow a_3 + a_4 .$$

The Lorentz invariant amplitude  $A$  can be written as a function of three variables

$$\left. \begin{aligned} s &= (p_1 + p_2)^2 = (p_3 + p_4)^2 = 4(k^2 + m^2) \geq 4m^2 \\ t &= (p_1 - p_3)^2 = (p_2 - p_4)^2 = -2k^2(1 - \cos\theta) \leq 0 \\ u &= (p_1 - p_4)^2 = (p_2 - p_3)^2 = -2k^2(1 + \cos\theta) \leq 0 \end{aligned} \right\} \quad (2.1)$$

satisfying the condition

$$s + t + u = 4m^2 \quad (2.2)$$

imposed by conservation of energy-momentum. Here, working in the centre of mass system,  $\theta$  is the scattering angle,  $k$  is the magnitude of 3-momentum,  $s$  is the square of total energy, and  $t, u$  are momentum transfers.

Two other physical scattering processes can be related to the  $s$ -channel reaction by crossing:

(1)  $t$ -channel scattering

$$a_1 + \bar{a}_3 \rightarrow \bar{a}_2 + a_4 ,$$

where  $\bar{a}_2, \bar{a}_3$  are antiparticles of  $a_2, a_3$  respectively.

The momenta of these antiparticles are given by

$$\left. \begin{aligned} p_{\bar{2}} &= -p_2 & , \\ p_{\bar{3}} &= -p_3 & . \end{aligned} \right\} \quad (2.3)$$

Here,  $t$  ( $t > 4m^2$ ) plays the role of energy variable and  $s, u$  ( $s, u \leq 0$ ) as momentum transfers.

(2)  $u$ -channel scattering

$$a_1 + \bar{a}_4 \rightarrow \bar{a}_2 + a_3 ,$$

where  $\bar{a}_2, \bar{a}_4$  are antiparticles with momenta

$$\left. \begin{aligned} p_{\bar{2}} &= -p_2 & , \\ p_{\bar{4}} &= -p_4 & . \end{aligned} \right\} \quad (2.4)$$

Here  $u$  ( $u \geq 4m^2$ ) is the energy variable and  $s, t$  ( $s, t \leq 0$ ) are momentum transfers.

The physical regions for the  $s$ -,  $t$ - and  $u$ -channels are separated from each other by an unphysical region which does not correspond to any physical process at all. To obtain a meaningful continuation of the amplitude from one region to another, Mandelstam<sup>7)</sup> postulated that  $A(s, t, u)$  is an analytic function of  $s, t$  and  $u$ . All discontinuities arise from bound states and physical cuts in this channel. Thus, except for possible subtractions,

$$\begin{aligned}
 A(s, t, u) = & \frac{1}{\pi} \int_{4m^2}^{\infty} ds' \frac{\rho_1(s')}{s'-s} + \frac{1}{\pi} \int_{4m^2}^{\infty} dt' \frac{\rho_2(t')}{t'-t} + \\
 & \frac{1}{\pi} \int_{4m^2}^{\infty} du' \frac{\rho_3(u')}{u'-u} + \frac{1}{\pi^2} \int_{4m^2}^{\infty} \int_{4m^2}^{\infty} ds' dt' \frac{\rho_{12}(s', t')}{(s'-s)(t'-t)} + \\
 & \frac{1}{\pi^2} \int_{4m^2}^{\infty} \int_{4m^2}^{\infty} dt' du' \frac{\rho_{23}(t', u')}{(t'-t)(u'-u)} + \\
 & \frac{1}{\pi^2} \int_{4m^2}^{\infty} \int_{4m^2}^{\infty} du' ds' \frac{\rho_{31}(u', s')}{(u'-u)(s'-s)}. \quad (2.5)
 \end{aligned}$$

The one dimensional integrals arise from Feynman graphs with single particle intermediate states. The double integrals arise from intermediate configurations where two or more particles are present in all three channels.

An extensive discussion on the evaluation of these double spectral functions and their boundary curves can be found in Reference<sup>8)</sup>. In terms of  $s$  and  $\theta$  :

$$A(s, \theta) = \frac{1}{\pi} \int ds' \frac{\rho_1(s')}{s' - s} + \frac{1}{\pi} \int dt' \frac{A_t(s, t', 4m^2 - s - t')}{t' + 2k^2(1 - \cos\theta)} + \frac{1}{\pi} \int du' \frac{A_u(s, 4m^2 - s - u', u')}{u' + 2k^2(1 + \cos\theta)} \quad (2.6)$$

where

$$A_t(s, t, u) = \rho_2(t) + \frac{1}{\pi} \int ds' \frac{\rho_{12}(s', t)}{s' - s} + \frac{1}{\pi} \int du' \frac{\rho_{23}(u', t)}{u' - u} \quad (2.7)$$

$$A_u(s, t, u) = \rho_3(t) + \frac{1}{\pi} \int ds' \frac{\rho_{31}(u, s')}{s' - s} + \frac{1}{\pi} \int dt' \frac{\rho_{23}(u, t')}{t' - t} \quad (2.8)$$

The discontinuity  $A_t$  can be written as a sum

$$A_t(s, t, u) = V_s^t(s, t, u) + A_t^{s(el)}(s, t, u) \quad (2.9)$$

$$A_t^{s(el)}(s, t, u) = \frac{1}{\pi} \int ds' \frac{\rho_{12}^{s(el)}(s', t)}{s' - s} \quad (2.10)$$

where  $\rho_{12}^{s(el)}$  is the contribution to  $\rho_{12}$  from elastic intermediate states in the  $s$ -channel and  $V_s^t$  is the 'generalized potential',<sup>7,8)</sup> for the  $s$ -channel generated

by the t-channel. Similarly

$$A_u(s,t,u) = V_s^u(s,t,u) + A_u^{s(el)}(s,t,u) \quad (2.11)$$

$$A_u^{s(el)}(s,t,u) = \frac{1}{\pi} \int ds' \frac{\rho_{3l}^{s(el)}(u,s')}{s' - s} \quad (2.12)$$

with  $V_s^u$  playing the role of generalized potential for the s-channel generated by the u-channel. Once  $V_s^t, V_s^u$  are given, the scattering amplitude  $A(s,\theta)$  can be solved completely.

The usual representation for partial wave amplitude with orbital angular momentum  $l$  is

$$A(s) = \frac{\eta(s)e^{2i\delta(s)} - 1}{2i\rho(s)} \quad , \quad (2.13)$$

$$\rho(s) = \sqrt{\frac{s-4}{s}} \quad , \quad (2.14)$$

giving

$$\text{Im } A(s) = \rho(s)|A(s)|^2 + \frac{1 - \eta^2(s)}{4\rho(s)} \quad . \quad (2.15)$$

Here  $\eta$  ( $0 \leq \eta \leq 1$ ) is the inelasticity parameter,  $\delta$  is the real part of phase shift and  $\rho(s)$  is a kinematical factor. The units used will be  $\hbar=c=1$ . Comparing this with the partial wave projection for  $A(s,\theta)$  in Equation (2.6) and using Equations (2.9) and (2.10), the imaginary parts of  $A(s)$  are

$$\text{Im } A^P(s) = \rho(s)|A(s)|^2 = \frac{1}{2\pi} \int_{-1}^1 d \cos\theta P_l(\cos\theta) \times \\ \left\{ \int dt' \frac{\text{Im } A_t^{s(el)}(s,t',4m^2-s-t')}{t' + 2k^2(1 - \cos\theta)} + \int du' \frac{\text{Im } A_u^{s(el)}(s,4m^2-s-u',u')}{u' + 2k^2(1 + \cos\theta)} \right\} \quad (2.16)$$



on the unitarity cut P ( $4m^2 \leq s \leq \infty$ ),

$$\begin{aligned}
 \text{Im } A^{\text{I}}(s) &= \frac{1 - \eta^2(s)}{4\rho(s)} \\
 &= \rho_1(s) \delta_{\ell,0} + \frac{1}{2\pi} \int_{-1}^1 d \cos\theta P_\ell(\cos\theta) \times \\
 &\quad \left\{ \int dt' \frac{\text{Im } V_s^t(s, t', 4m_2^2 - s - t')}{t' + 2k^2(1 - \cos\theta)} \right. \\
 &\quad \left. + \int du' \frac{\text{Im } V_s^u(s, 4m_2^2 - s - u', u')}{u' + 2k^2(1 + \cos\theta)} \right\} \quad (2.17)
 \end{aligned}$$

on the inelastic cut I ( $s_I \leq s \leq \infty$ ) with threshold  $s_I$ ,  
and

$$\begin{aligned}
 \text{Im } A^{\text{U}}(s) &= -\frac{1}{2} \int_{-1}^1 d \cos\theta P_\ell(\cos\theta) \{ \text{Re } A_t [4(k^2 + m^2), - \\
 &\quad 2k^2(1 - \cos\theta), -2k^2(1 + \cos\theta)] + \\
 &\quad \text{Re } A_u [4(k^2 + m^2), -2k^2(1 - \cos\theta), -2k^2(1 + \cos\theta)] \} \\
 &\quad (2.18)
 \end{aligned}$$

on the unphysical cut U ( $-\infty \leq s \leq 4m^2$ ).

The discontinuities  $A_t$ ,  $A_u$  are made up of contributions from different kinds of intermediate states, and  $\text{Im } A^{\text{U}}(s)$ ,  $\text{Im } A^{\text{I}}(s)$  are similarly composed of additive parts. For example, an intermediate state of mass  $\mu$  in the t- or u-channel would give a non-zero contribution to  $\text{Im } A^{\text{U}}(s)$  in the interval  $s = -\infty$  to  $(4m^2 - \mu^2)$ . Thus one

expects the least massive particles which produce the longest range forces to dominate the nearby region of the  $s$ -axis below the physical threshold. As one goes farther and farther to the left more and more massive particles which produce shorter range forces enter the picture as well. This result is very useful. It implies that low energy scattering is dominated by the longest range, much better known forces; the shorter range, less understood forces can be taken into account approximately by a few parameters such as cut-offs and/or distant poles.

### 3. EQUATIONS

We shall consider the S- and P-wave scattering of two unit mass, pion-like particles in the centre of mass system with the partial wave amplitude given by Equation (2.13),

$$A(s) = \frac{\eta(s) e^{2i\delta(s)} - 1}{2i\rho(s)} . \quad (2.13') \quad (3.1)$$

This amplitude can be written as a sum of Cauchy integrals over the unitarity cut  $P$ , inelastic cut  $I$  and unphysical cut  $U$ ,

$$A(s) = A^P(s) + A^I(s) + A^U(s) . \quad (3.2)$$

If one writes

$$A(s) = \frac{N(s)}{D(s)} \quad (3.3)$$

and proceed to solve the N/D integral equations for  $A(s)$ , the threshold condition

$$\delta_{\ell} \propto k^{2\ell+1} \quad (3.4)$$

is not satisfied for  $\ell \geq 1$ . To ensure the correct threshold behaviour, we follow the Frye and Warnock prescription<sup>8)</sup> by constructing a new amplitude

$$\tilde{A}(s) \equiv \theta(s) A(s) = \frac{\theta(s)N(s)}{D(s)} \quad (3.5)$$

$$\theta(s) = (s - 4)^{-\ell} \quad (3.6)$$

and proceed to solve the integral equations for  $[\theta N]$  and  $D$ . Choosing the phase  $D(s)$  in any partial wave as

$$\frac{D^*(s)}{D(s)} = e^{2i\delta(s)}, \quad s \geq 4, \quad (3.7)$$

one has

$$\text{Im } D(s) = - \frac{2\rho(s)}{1+\eta(s)} \text{Re } N(s), \quad s \geq 4, \quad (3.8)$$

$$\text{Im } N(s) = \frac{1 - \eta(s)}{2\rho(s)} \text{Re } D(s), \quad s \geq s_I, \quad (3.9)$$

and on the unphysical cut  $U$ ,

$$\text{Im } N(s) = D(s) \text{Im } A(s). \quad (3.10)$$

The integral equations for  $[\theta N]$  and  $D$  are as follows

$$\theta(s)N(s) = \frac{1}{\pi} \int_U \frac{\theta(s')D(s')\text{Im } A(s')}{s' - s} ds' +$$

$$\frac{1}{\pi} \int_I \frac{\theta(s')}{s' - s} \left[ \frac{1 - \eta(s')}{2\rho(s')} \text{Re } D(s') \right] ds' \quad (3.11)$$

and

$$D(s') = 1 + \frac{s - s_0}{\pi} \int_P \left[ -\frac{2\rho(s')}{1 + \eta(s')} \text{Re } N(s') \right] \frac{ds'}{(s' - s)(s' - s_0)} .$$

(3.12)

A subtraction has been made on the D function at the symmetry point  $s_0 = \frac{4}{3}$ . On substituting Eq. (3.12) into (3.11) and reversing the order of integration,

$$\frac{2\eta(s)}{1 + \eta(s)} [\theta(s)\text{Re } N(s)] = \theta(s)\tilde{B}(s) + \frac{1}{\pi} \int_P \left[ \frac{2\theta^{-1}(s')\rho(s')}{1 + \eta(s')} \times \right.$$

$$\left. \theta(s')\text{Re } N(s') \right] \left[ \frac{(s' - s_0)\theta(s')\tilde{B}(s') - (s - s_0)\theta(s)\tilde{B}(s)}{(s' - s)(s' - s_0)} \right] ds'$$

$s > 4$  , (3.13)

where

$$\theta(s)\tilde{B}(s) = \frac{1}{\pi} \int_U \frac{\theta(s')\text{Im } A(s')}{s' - s} ds' + \frac{1}{\pi} \int_I \frac{\theta(s')}{s' - s} \left[ \frac{1 - \eta(s')}{2\rho(s')} \right] ds' .$$

(3.14)

The resonance width, with kinematical factors included, is obtained from the Breit-Wigner form

$$\lim_{s \rightarrow s_R} A(s) \propto \frac{1}{(E_R - E) - \frac{i}{2} \Gamma} \quad (3.15)$$

to give

$$\Gamma = - \frac{\sqrt{s-4}}{s(1+\eta)} \left. \frac{\operatorname{Re} N}{\frac{d \operatorname{Re} D}{ds}} \right|_{s=s_R} \quad (3.16)$$

where  $s_R$  is the resonance position defined as the energy where  $\delta$  rises through  $90^\circ$ .

The potentials chosen are such that one can solve the dispersion relations analytically when elastic unitarity is employed. For the S wave ( $l=1$ ,  $\theta=1$ ) the model is that of scattering by two exponential potentials,

$$\frac{1}{\pi} \int_U \frac{\operatorname{Im} A(s')}{s' - s} ds' = \sum_{i=1}^2 \frac{\lambda_i}{s + s_i} \quad (3.17)$$

with  $\lambda_i$ ,  $s_i$  chosen to give a short range attraction with a repulsive barrier. In the P wave [ $l=1$ ,  $\theta(s)=(s-4)^{-1}$ ] a single pole is used

$$\frac{1}{\pi} \int_U \frac{\theta(s') \operatorname{Im} A(s')}{s' - s} ds' = \frac{\lambda_1}{s + s_1} \quad (3.18)$$

To avoid divergence difficulties, the inelastic parameter used is a step function with rounded edges, i.e.

$$\eta(s) = \begin{cases} 1 - \alpha + \alpha \cos\left(\frac{s-a}{\Delta} \pi\right), & a < s < a + \Delta \\ 1 - 2\alpha & , a + \Delta \leq s \leq b - \Delta \\ 1 - \alpha + \alpha \cos\left(\frac{b-s}{\Delta} \pi\right), & b - \Delta < s < b \\ 1 & , \text{otherwise} \end{cases} \quad (3.19)$$

#### 4. RESULTS AND DISCUSSIONS

An elastic resonance at an arbitrary point  $s_R=25$  was secured by adjusting the pole parameters  $\lambda_1, s_1$ . With these parameters fixed, three separate cases with  $s_R$  (a) above the inelastic region (region where  $\eta(s) \neq 1$ ), (b) embedded in the inelastic region, and (c) below the inelastic region were studied. The results were as follows:

##### S wave

The choice of parameters that gave an elastic resonance at  $s_R=25$  was  $\lambda_1 = -500$ ,  $\lambda_2 = 3228.7$ ,  $s_1 = 150$ ,  $s_2 = 2000$ . Inelasticity was then switched on and the following three situations were studied:

(a)  $b < s_R$  (Figure 1)

We found that inelasticity switched on and off below  $s_R$  decreased the resonance mass and reduced its width; weaker inelasticity made these effects less pronounced.

(b)  $a < s_R < b$  (Figure 2)

With the parameters used, the results were similar to case (a).

(c)  $a > s_R$  (Figure 3)

If  $\eta$  was sufficiently different from unity, double resonances were produced - one (denoted by  $R_1$ ) below  $s_R$  and the other ( $R_2$ ) above it. Compared with the original

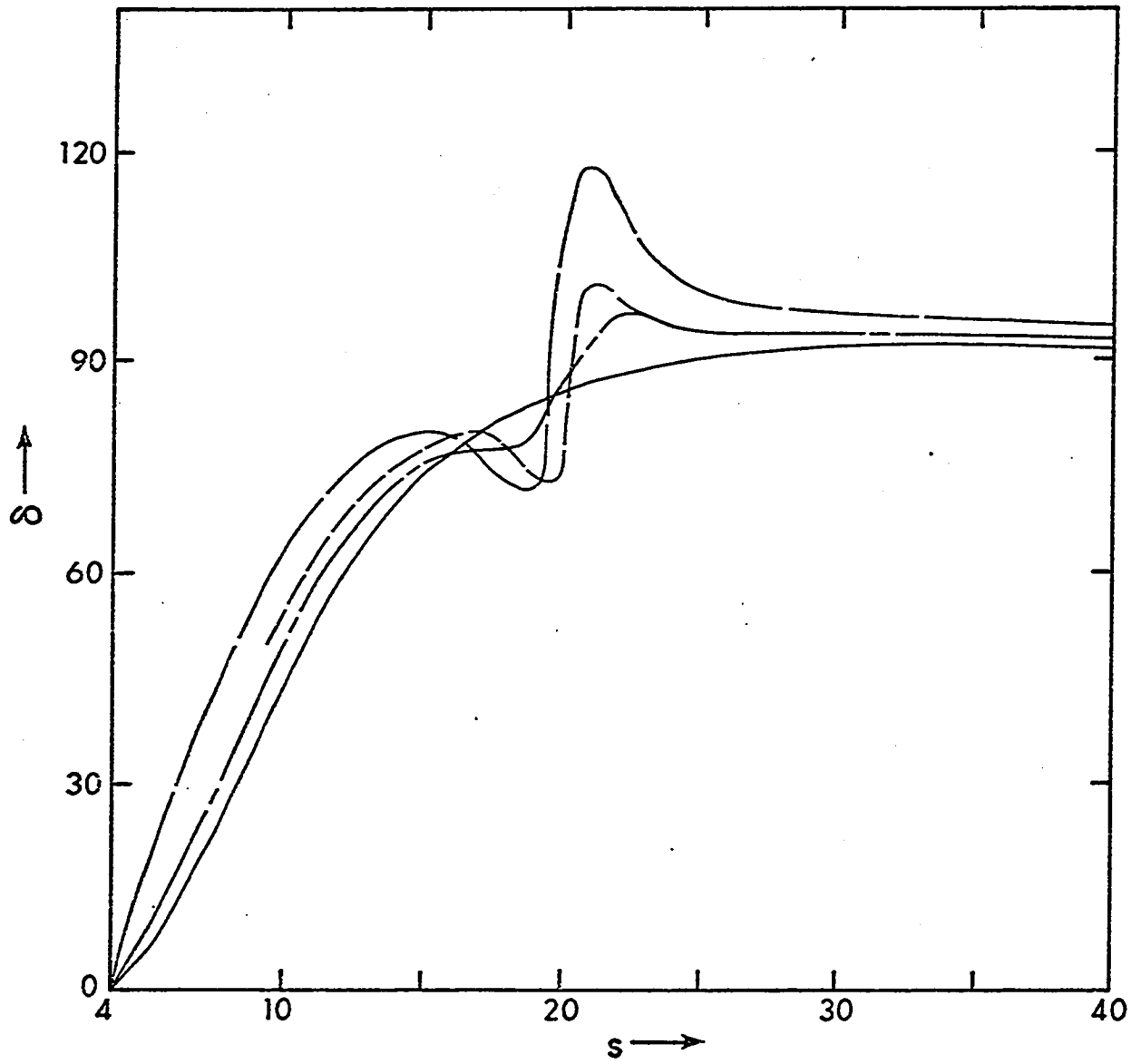


Figure 1

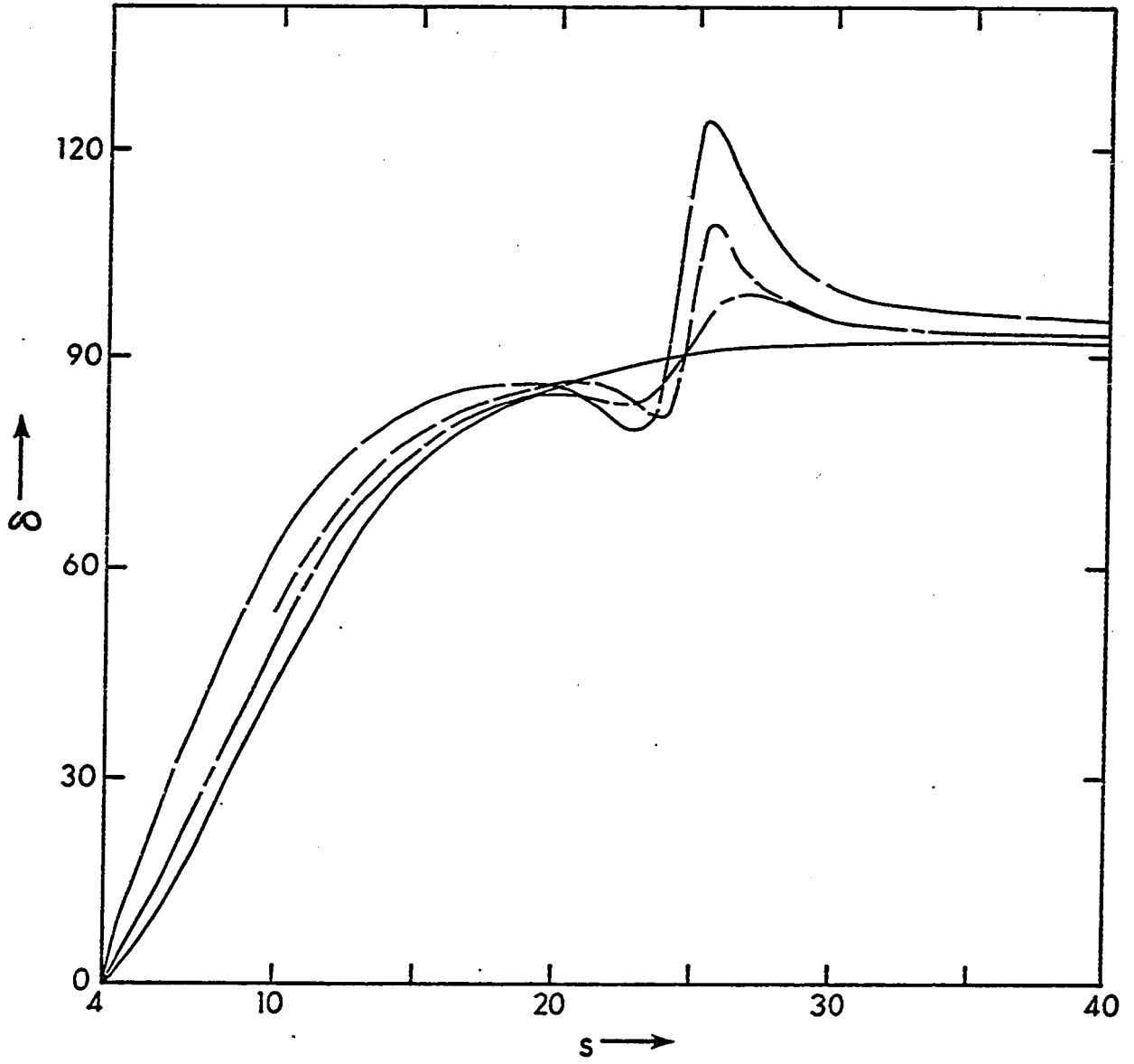


Figure 2



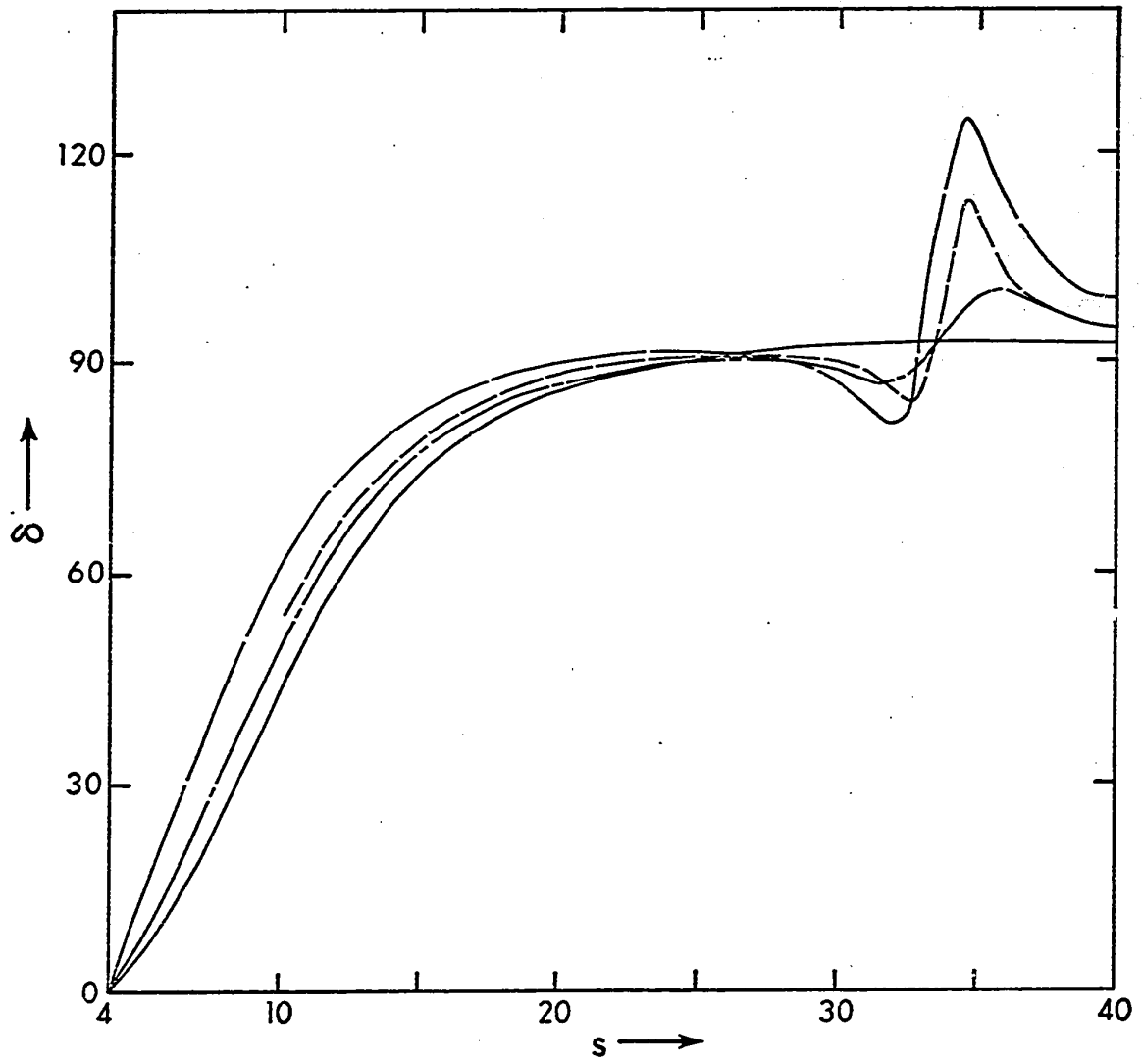


Figure 3

resonance,  $R_2$  had a smaller width whereas  $R_1$  had a larger width. It was also found that  $R_1$  disappeared if the extent by which  $\eta$  departed from unity was reduced.

### P wave

The parameters used to give a resonance at  $s_R=25$  were  $\lambda_1=2.515$ ,  $s_1=100$ .

(a)  $b < s_R$  (Figure 4)

We found that a weak inelasticity ( $\eta \approx 1$ ) increased the resonance mass and decreased its width; stronger inelasticity enhanced these effects and at the same time produced a second resonance (denoted by  $R_1$ ) below  $s_R$ . A narrower inelastic region had the two resonances closer together.

(b)  $a < s_R < b$  (Figure 5)

It was found that the general features were very much similar to case (a). In the examples given, double resonances were obtained.

(c)  $s_R < a$  (Figure 6)

Double resonances were obtained if  $\eta \approx 1$  in a narrow region. The higher mass resonance disappeared if the width of this region was increased, or the value of  $\eta$  differed considerably from unity.

From the definition of generalized potential and the Ball-Frazer mechanism<sup>9)</sup>, one expects the inelastic

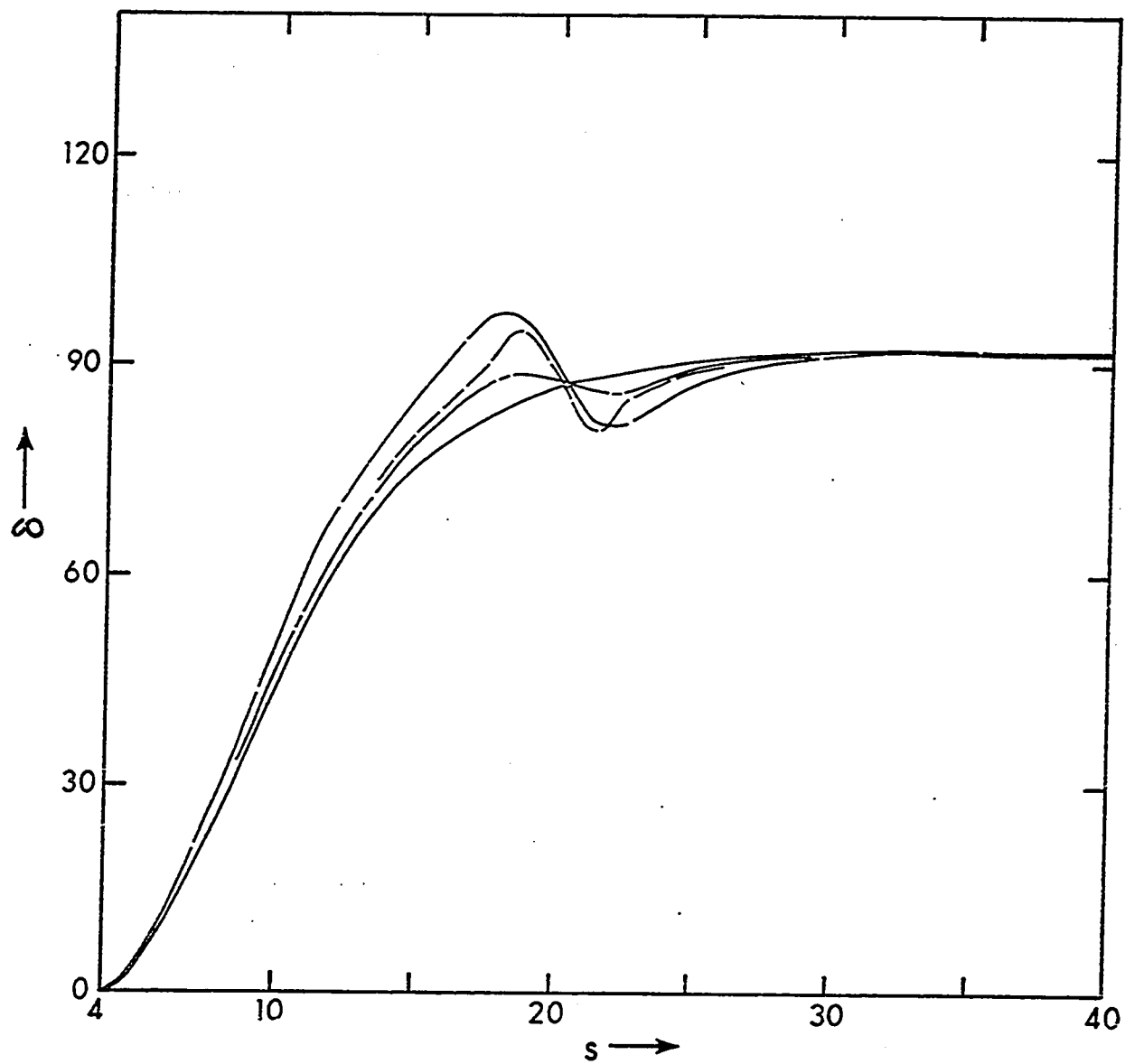


Figure 4

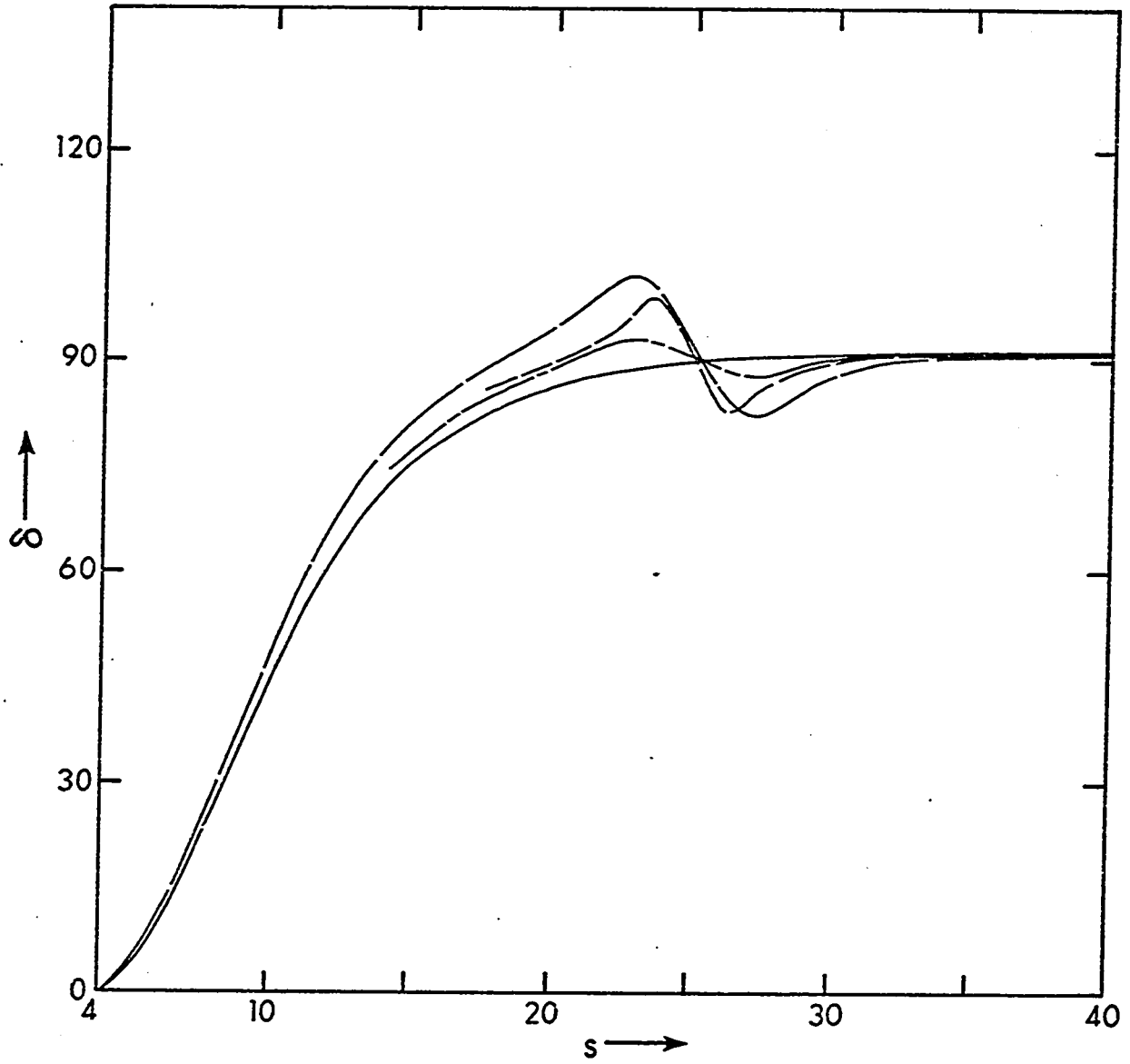


Figure 5

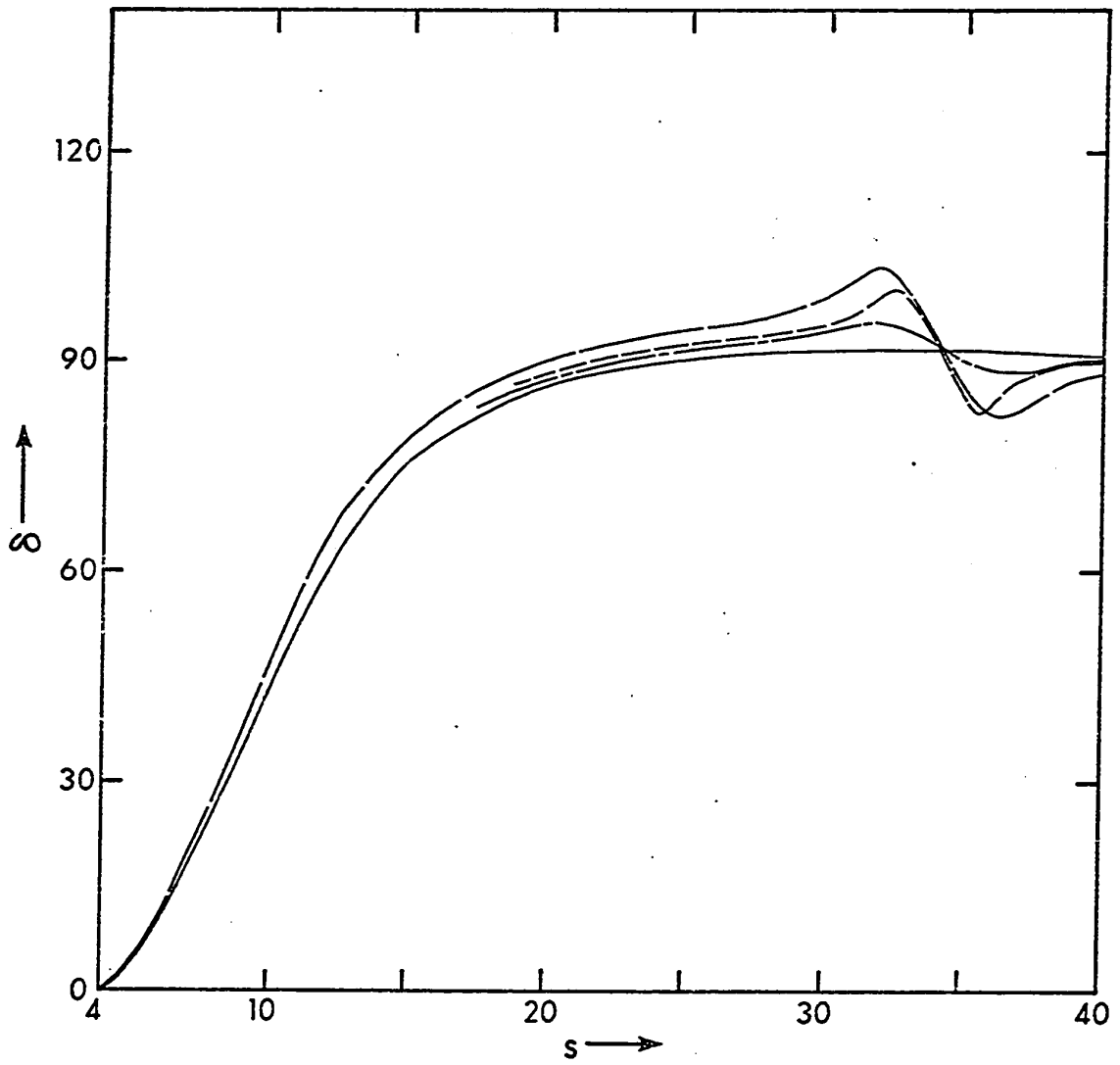


Figure 6

channels to produce an energy dependent potential which is attractive below the region where  $\eta \neq 1$  ( $s < a$ ) and repulsive above it ( $s > b$ ). If the elastic potential is monotonic, as is the case in the P-wave problem, the total potential at energies  $s < a$  would be more attractive and thus if there was an elastic resonance at  $s_R < a$  one would expect it to move toward the elastic threshold. On the other hand if the elastic resonance was at an energy  $s_R > b$  then one would expect it move away from the elastic threshold.

The Ball-Frazer mechanism also indicates that the effect of inelasticity in a limited energy region is to put a wiggle on the phase shift. This is demonstrated in Figure 7 where the phase shift has been sketched for the case where inelasticity alone 'drives' the reaction. The wiggle may be large enough in certain cases, in particular for broad resonances, to take the phase shift through  $90^\circ$ , bring it down below  $90^\circ$  and finally take it up through  $90^\circ$  again as the energy increases, thereby producing double resonances.

Our results for the P-wave problem bear out this intuitive picture. The centrifugal barrier provides the resonance trapping mechanism. The elastic potential is attractive and monotonic. The results of the S-wave

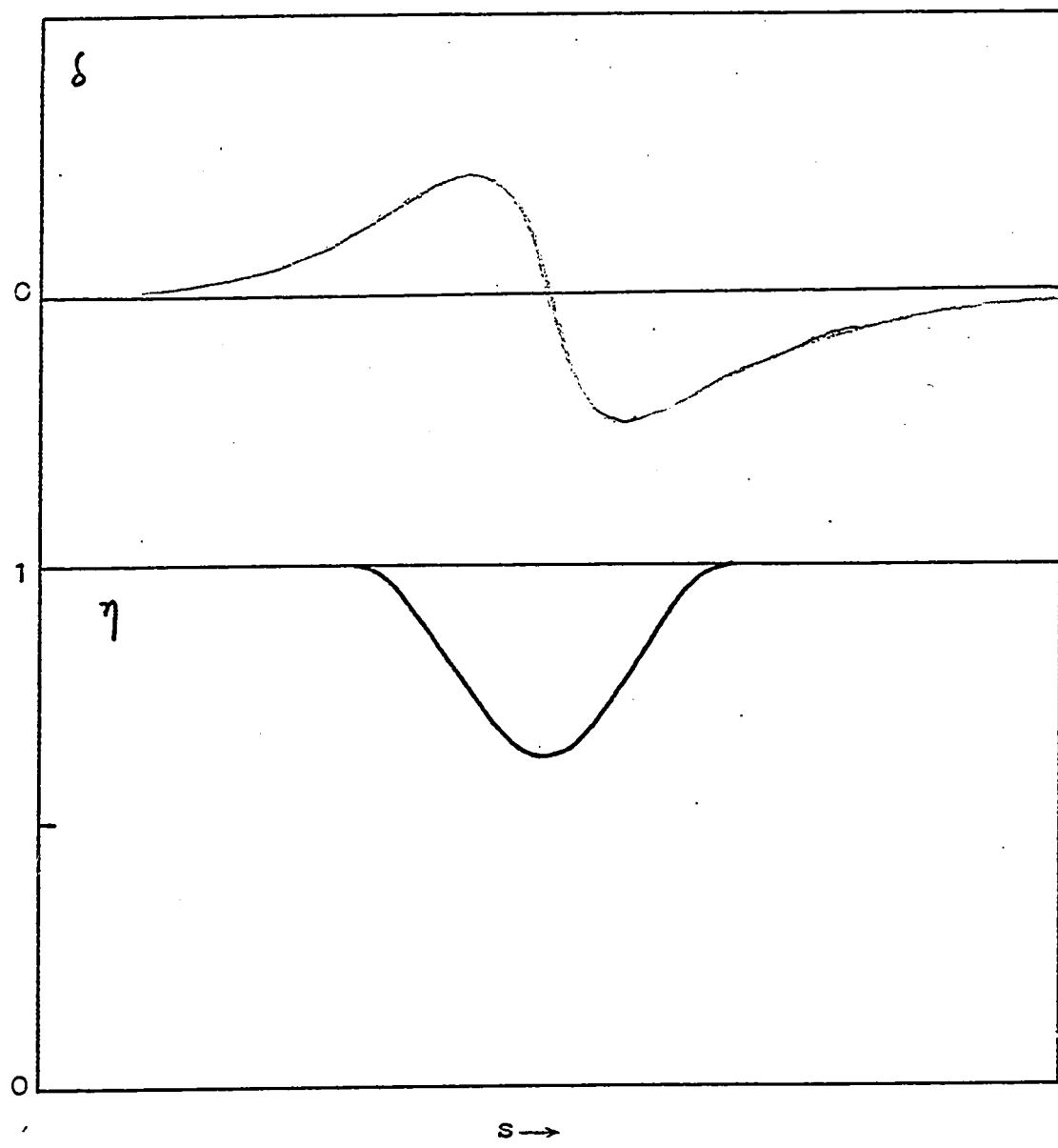


Figure 7

problem however demonstrate that the intuitive picture which worked so well for the P-wave breaks down. The reason probably is that the S-wave potential used was not monotonic. A repulsive barrier (with a relatively short range) was provided to trap the resonance and it is not so clear as to how one should expect the resonance to behave once inelasticity is switched on.



## REFERENCES

1. G.F. Chew, F.E. Low, Phys. Rev. 101 (1956) 1570;  
G.F. Chew, M.L. Goldberger, F.E. Low and  
Y. Nambu, Phys. Rev. 106 (1957) 1337;  
J.S. Ball and D.Y. Wong, Phys. Rev. 133  
(1964) B179; 138 (1965) AB4(E).
2. F. Zachariasen, Phys. Rev. Letters 7 (1961) 112, 268.
3. J. Fulco, G.L. Shaw and D.Y. Wong, Phys. Rev. 137  
(1965) B1242.
4. M. Der Sarkissian and P. Nath, Nuovo Cimento 38  
(1965) 1355.
5. P.W. Coulter and G.L. Shaw, Phys. Rev. 138 (1965)  
B1273.
6. M. Bander, P.W. Coulter and G.L. Shaw, Phys. Rev.  
Letters 14 (1965) 270.
7. S. Mandelstam, Phys. Rev. 112 (1958) 1344; 115 (1959)  
1741, 1752.
8. G.F. Chew and S.C. Frautchi, Phys. Rev. 124 (1961) 264;  
G.F. Chew, S-Matrix Theory of Strong Interactions  
(W.A. Benjamin, Inc., New York, 1962)(Chapter 7);  
S.C. Frautchi, Regge Poles and S-Matrix Theory  
(W.A. Benjamin, Inc., New York, 1963)(Chapter 6).
9. G. Frye and R.L. Warnock, Phys. Rev. 130 (1963) 478.